Comparison of the Knee-Thigh-Hip Response in Small Female ATDs with Female PMHS

Randolff L. Carpenter, Parker R. Berthelson, John-Paul Donlon, Jason L. Forman

Abstract Bilateral knee impacts were conducted on Hybrid III and THOR 5th percentile female anthropomorphic test devices (ATDs), and the results were compared to previously reported female PMHS data. Each ATD was impacted at velocities of 2.5, 3.5, and 4.9 m/s. Knee-Thigh-Hip (KTH) loading data, obtained either via direct measurement or through exercising a one-dimensional Lumped Parameter Model (LPM), was analysed for differences in loading characteristics including the maximum force, time to maximum force, loading rate, and loading duration. The ATDs displayed higher loading rates and maximum forces, and the lowest loading duration and time to peak force for each point along KTH compared to the PMHS. The force transfer from the knee to the femur was 79.4 ± 2.4% for the Hybrid III 5th female, 82.7 ± 0.4% for the THOR-05F, and 70.6 ± 1.7% for the PMHS. The force transfer from the knee to the hip was 60.6 ± 0.4% for the Hybrid III 5th female, 41.4 ± 0.4% for the THOR-05F, and 57.0 ± 3.0% for the PMHS. Contextualizing the results with data from epidemiology studies suggests that while maximum force may be a useful parameter in analysing KTH force transfer, the force transfer behaviour of the PMHS and ATDs were not uncharacteristic from what was estimated via simple scaling techniques using mid-size male subjects. Thus, the authors explored additional factors which may contribute to the injury patterns in the field data but were not explored in the current study and should be addressed in future work.

Keywords Female, Frontal Impacts, Knee-Thigh-Hip, Lumped-Parameter Modelling, ATDs.

I. INTRODUCTION

Injuries to the lower extremities during frontal collisions, although not necessarily fatal, can have substantial implications on the quality of life for an individual. One load path of particular concern is along the Knee-Thigh-Hip (KTH) complex, accounting for 25% of all life-years lost in frontal collisions, with the hip accounting for 65% of that value [2]. One mechanism for this type of loading comes from occupant interaction with the lower instrument panel, where the force initiates at the knee and then travels along the femur before reaching the hip. Determining the force transfer along KTH poses a challenge when seeking to develop countermeasures to mitigate these injuries, as the force decreases as it is expended by the acceleration of the increasingly recruited mass along the KTH load path.

One method for analysing the force along KTH involves the combined approach of experimental testing and modelling. Through bilateral knee impact tests on mid-sized male post-mortem human subjects (PMHS), Rupp and co-authors were able to generate a one-dimensional lumped parameter model (LPM) detailing the force transfer along KTH [3]. By performing simulations with the model, it was calculated that the force transfer from the knee to the hip was 53.7±0.9% of the initially applied force at the knee. While this proved a key advancement in understanding KTH force transfer, the applicability of the model for a more diverse subject population was unproven. More specifically, the effect of sex on KTH force transfer has not been explored. In an epidemiology study by [4],the authors determined that females were 1.89 times more likely to sustain an injury to KTH, even after controlling for relevant crash characteristics, and the cause of this difference in risk remains unknown. Similar conclusions were also drawn by [5] in a later investigation.

To study the effect of sex on KTH force transfer, [1] conducted a series of bilateral knee impact tests on female PMHS, employing methods that were similar to what was done previously with males. The authors used the results from testing to develop an updated LPM for females where it was estimated that 57.0±3.0% was transferred to the hip. While this was an important first step in the understanding of KTH force transfer for females, the next major challenge involves determining the relationship between the KTH behaviour in female PMHS and the behaviour in small female anthropomorphic test devices (ATDs). Knowledge of this relationship helps in the creation of a transfer function between subjects for use in vehicle safety tests or for future efforts

R. L. Carpenter is a PhD student (phone: 434-297-8009, email: rlc4gj@virginia.edu), P. R. Berthelson is a Mechanical Engineer, J. P. Donlon is a Senior Research Specialist, and J. L. Forman is a Principal Scientist at the University of Virginia's Center for Applied Biomechanics in Charlottesville, Virginia.

at improving the biofidelity of the KTH response in female ATDs.

Therefore, the goal of this study was to compare the force transfer response for the Hybrid III 5th female ATD and the THOR 5th female ATD (THOR-05F) to the force transfer response for female PMHS reported previously [1]. To achieve this, the knees of the ATDs were bilaterally impacted using similar test conditions as reported in the PMHS tests [1]. While the data for obtaining the force transfer along KTH for the THOR-05F could be measured directly through experimental testing, complete quantification of the Hybrid III response required the development of an LPM. The loading characteristics and force transfer behaviour of the ATDs were then compared to those of the PMHS [1]. Kinematic responses were also analysed to determine if they had any effect on the force transfer.

II. METHODS

Experimental Testing

Detailed descriptions of the experimental test methodology were reported previously by [1] and are summarized here. An overview of the test setup is shown in Figure 1. At the start of each test, the subject was positioned in an upright seated posture (Fig. 2). Knee impacts were performed using a ram coupled to a pneumatically driven linear actuator that was servo-hydraulically controlled with active feedback (DSD, Linz, Austria). Impactor faces were padded with one layer of 1" thick 50 Durometer Sorbothane (Shore OO) affixed to another layer of 1" thick 70 Durometer Sorbothane (Shore OO) (Sorbothane Inc., Kent, Ohio)[3]. To record the force during each impact, 6-axis load cells (Model 3868TF, Robert A. Denton, Inc.) were mounted behind the padding. Load cells (Model M3255, Sunrise Instruments LLC) were also mounted under the seat and footplate of the test rig to measure each subject's interaction with the environment.

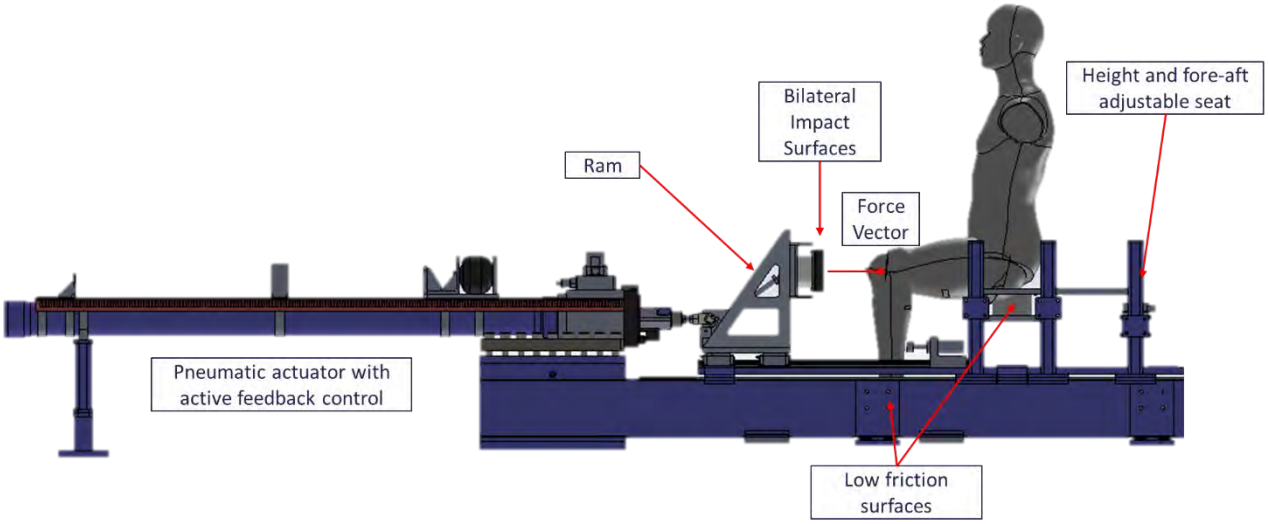

Fig. 1. Overview of test fixture. A pneumatic actuator linearly accelerated a ram with padded impact surfaces into the ATDs' knees while the ATDs sat on a low-friction seat and foot support.

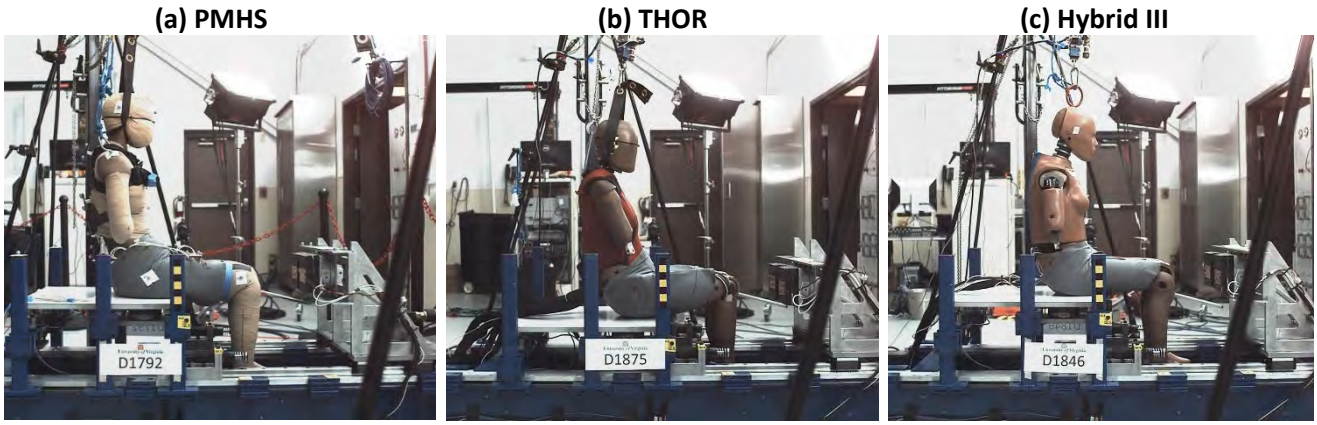

Fig. 2. Example setup for a) PMHS [1], b) THOR, and c) Hybrid III.

Subjects were impacted using target velocities of 2.5, 3.5, and 4.9 m/s (Table 1). Each pulse was designed so that the ram accelerated up to the desired target velocity, stopped accelerating, contacted the subject's knees, and then maintained that same velocity throughout the event. Testing was stopped after one 4.9 m/s impact for THOR due to damage observed in the knee slider. Damage was also observed to the Hybrid III ATD, though this occurred after all whole-body tests were completed. All data were acquired using a sampling rate of 10 kHz with the Slice Pro data acquisition system (Diversified Technical Systems Inc.). Data collected for all subjects included femur and pelvis, kinematics, and the force interaction with the test environment including bilateral force data from the load cells placed behind the impacting surface in contact with the knees, and friction data from load cells placed under the seat plate. All subject data is oriented in the anterior-to-posterior (AP) loading direction, corresponding to the x axis for the pelvis and the z axis for the femurs. The lone exception was the acetabular load cells unique to the THOR-05F ATD, in which the resultant load was used to remain consistent with regulatory testing. For the PMHS, femur kinematics were tracked by a sensor placed on the mid-shaft and transformed to the centre of the bone, pelvis kinematic were tracked via a pelvis mount attached to the posterior superior iliac spine (PSIS) which was then transformed to the centre of the hip joints using medical imaging data for reference. More detailed descriptions of the PMHS instrumentation and transformation methods can be found in [1]. Since femur kinematics are not a standard measurement obtainable by the ATDs, uniaxial accelerometers were placed on the left and right femur of the ATDs during testing, positioned along the local femur z axis. For the Hybrid III, the measurement was taken at the anterior-most portion of the femur due to a lack of available locations from the tight coupling of the flesh on the ATD. For THOR, the accelerometer was mounted on the Slice Nano structural replacement module attached to the femur bushing assembly. All measurements obtained via instrumentation in the test environment were filtered at CFC 60, whereas instrumentation installed inside the ATDs was filtered at CFC 180. Contact timing for each test was determined based on the time when the applied force was last below 0.5% of the maximum force. For the THOR ATD, femur and hip loading data were obtained directly through testing. For PMHS and Hybrid III tests, complete loading information along KTH required the use of computational methods.

TABLE I
SUMMARY OF TESTS PERFORMED

Impact Velocity (m/s)	Subject	Number of Tests
2.5	PMHS†	4
	THOR	3
	Hybrid III	3
3.5	PMHS†	4
	THOR	3
	Hybrid III	3
4.9	PMHS†	4
	THOR*	1
	Hybrid III	3

*Testing stopped after damage was observed to ATD
†PMHS tests were previously reported by [1]

Subjects

Experimental testing involved the use of the Hybrid III and THOR 5th percentile female ATDs, and four female PMHS. PMHS results were analysed and reported previously by [1], and were used as a source of comparison for the ATD response data. Table 2 presents the subject characteristics, including a comparison of the PMHS anthropometry with that of the ATDs. While the PMHS were all taller than the ATDs, the mass and body mass index (BMI) of each subject were consistent with the ATDs, except for PMHS 4, who had a lower mass and BMI than the ATDs.

TABLE II
SUBJECT CHARACTERISTICS

Subject	Sex	Age	Cause of Death	Stature (cm)	Mass (kg)	BMI (kg/m^2)
1	F	69	Amyotrophic Lateral Sclerosis	156	49.4	20.5
2	F	48	Blunt Force Chest Trauma	165	59.0	21.8
3	F	46	End Stage Renal Disease	156	51.3	21.1
4	F	70	Acute Respiratory Failure	172	45.4	15.4
Average PMHS				162 (±8)	51.3 (±5.7)	19.7 (±2.9)
Hybrid III 5th Percentile Female ATD				150	49.0	21.8
THOR-05F ATD				151	47.5	20.8

Positioning

The primary focus of dummy positioning was to achieve the neutral, upright seating posture that was first defined in previous studies for female PMHS, mid-size male PMHS, and mid-size male ATD tests [1,3]. Positioning measurements are shown in Table III for the aforementioned female PMHS [1] as well as the current ATDs. To achieve an upright seated posture in the Hybrid III, the ATD was hoisted by a drop release mechanism connected to a rope and ring mount attached on the Hybrid III head. For THOR, a head strap, connected to the drop release, was used to support the head under the chin. Once upright, the ATDs were adjusted such that their positioning relative to the ram was consistent with the PMHS (padding-to-knee distance), their knee angles were approximately 90-degrees to minimize the effects of flexion/extension, and their knee centres were approximately in line with the acetabulum to minimize the effects of abduction/adduction. ATD measurements were consistent with the PMHS, except for the recline and tilt angles measured by tilt sensors in the THOR ATD which showed slight posterior rotation. During each test, the drop release mechanism released upon trigger, leaving the subjects unconstrained during the impact. Similar to the female PMHS tests [1], a slacked support rope was used to catch the subject after the event of interest had concluded and was not determined to play a role in the knee impact based off an analysis of high speed video.

TABLE III
MEASURED POSITIONING PARAMETERS

Measurement	Units	Target	Subject 1 [1]	Subject 2 [1]	Subject 3 [1]	Subject 4 [1]	Hybrid III	THOR
Recline Angle	Deg	0.0 ± 5.0	0.2 ± 1.5	-0.1 ± 0.5	-0.8 ± 1.2	-0.1 ± 0.5	-0.8 ± 0.4	13.7 ± 0.7
Pelvic Tilt Angle	Deg	0.0 ± 5.0	-0.9 ± 0.7	-2.0 ± 0.4	-1.0 ± 1.5	0.8 ± 0.4	--	16.2 ± 1.0
Left Knee Angle	Deg	90.0 ± 5.0	89.8 ± 1.0	89.4 ± 0.7	90.9 ± 1.3	87.9 ± 2.4	92.2 ± 1.0	88.7 ± 0.8
Right Knee Angle	Deg	90.0 ± 5.0	92.8 ± 1.1	89.4 ± 0.5	90.3 ± 2.2	87.0 ± 2.9	91.3 ± 0.7	88.6 ± 0.8
Knee Centre-to-Centre	mm	*	165 ± 2	203 ± 1	179 ± 2	168 ± 2	177 ± 3	200 ± 4
Left Padding-to-Knee	mm	178 ± 5	178 ± 3	177 ± 2	178 ± 3	176 ± 1	177 ± 3	178 ± 2
Right Padding-to-Knee	mm	178 ± 5	179 ± 2	176 ± 2	178 ± 3	176 ± 2	177 ± 2	177 ± 2

Lumped Parameter Modelling

For the PMHS and the Hybrid III ATD, hip forces were not directly measurable, and hence were unobtainable without employing computational methods. Figure 3 shows the LPM that was developed previously for simulating the subject-specific responses of female PMHS to bilateral knee loading, along with the corresponding model definitions in Table III [1]. The complete set of parameters used for each simulation of the PMHS LPMs are shown in Table A1 of the appendix. To obtain the LPM for the Hybrid III ATD, whole-body mass scaling techniques were employed. Using the whole-body mass of the Hybrid III 50th male (m_{50M}), and the

whole-body mass of the Hybrid III 5th percentile female (m_{05F}), Equation 1 was used to calculate the scale factor (λ_m).

$$\lambda_m = \frac{m_{05F}}{m_{50M}} \quad (1)$$

After obtaining the scaling factor, the final LPM mass values reported by [6] were scaled to obtain the LPM for Hybrid III (Table B1). The force-time history recorded at the knee for each impact was then used to simulate each of the LPMs over a 40 ms duration following the impact. The only output Hybrid III value that was used for comparison in this study includes the predicted loading response at the hip. For each set of tests, the model was validated by comparing the femur force, femur acceleration, and pelvis acceleration data measured by the Hybrid III ATD with the same measurements predicted in the model (Fig. B1-B5).

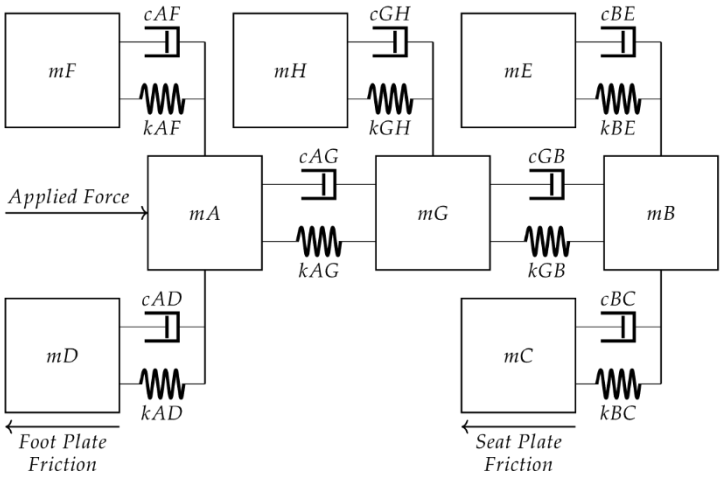

Fig. 3. Lumped parameter model developed to characterize the force transfer along knee-thigh-hip. Variables correspond to different regions of KTH and include the masses, stiffness, and damping, as well as the frictional interactions between masses.

TABLE III
LUMPED PARAMETER MODEL MASS DEFINITIONS

Variable	Mass Definition
mA	Distal femur, knee, and knee flesh
mB	Pelvis
mC	Pelvis flesh
mD	Lower legs (below the knee)
mE	Upper body (above pelvis)
mF	Thigh flesh coupled to distal femur
mG	Proximal femur
mH	Thigh flesh coupled to proximal femur

Following the completion of the simulations, force data that was either measured or predicted were further analysed to determine the loading characteristics at the knee, femur, and hip across the different subjects. Characteristics include the maximum load, time to maximum load, loading rate, loading duration, and impulse of loading, with definitions consistent with those described in previous studies [1,3]. Finally, the force transfer of each model was evaluated to determine the percentage of force transferred to the femur and hip relative to the initial load applied at the knee.

III. **RESULTS**

Input Loading

The input force measured from the bilateral knee load cells on the ram was averaged for each ATD, and the behaviours were compared to the results obtained from the PMHS experimental tests (Fig. 4) [1]. The knee loading traces for the ATDs matched each other more than they matched the PMHS. In particular, the THOR-05F responses, especially at the lower impact speeds, were so repeatable that the standard deviation corridors in the figures are often not visible. Knee loading characteristics were then calculated and analysed for trends between the different subjects at varying impact velocities (Appendix C). Across all impact velocities, the Hybrid

III ATD had the largest loading rate and maximum force, while also having the shortest time to peak force and loading duration. Conversely, the PMHS had the smallest loading rate and maximum force and the longest time to peak force and loading duration. Knee impulses across all subjects were consistent and increased with increasing impact velocity.

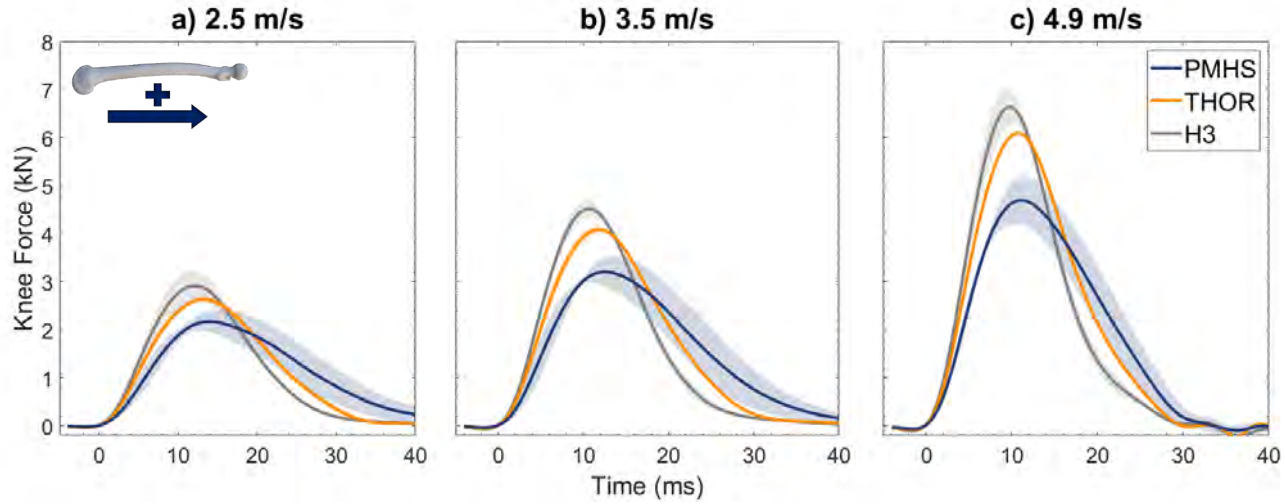

Fig. 4. Average knee impact force measured for PMHS, THOR, and Hybrid III (± one standard deviation) for impact velocities of a) 2.5 m/s, b) 3.5 m/s, and c) 4.9 m/s. Positive knee force is directed along the long axis of the femur in the distal-proximal direction.

Femur Kinematics

Femur acceleration-time histories are shown in Figure 5, with anterior-to-posterior (A-P) femur acceleration representing a positive value. Additional femur kinematic data can be found in Appendix D. Maximum femur acceleration for the two ATDs occurred simultaneously, and the average magnitude of maximum femur acceleration differed between the two ATDs by 2.3 g, 2.8 g, and 0.9 g for each respective impact velocity. Further, the shape of the ATD curves matched closely, with the exception of a gap between the responses occurring around 20 ms after impact, after the femurs reached their maximum values. In comparison, PMHS femur accelerations peaked at an earlier time than the ATDs, averaging 7.9 ± 2.1 ms for 2.5 m/s impacts, 6.1 ± 1.5 ms for 3.5 m/s impacts, and 5.6 ± 0.7 ms for 4.9 m/s impacts. Finally, despite an earlier peak, the maximum femur accelerations for the PMHS were similar in magnitude to the ATDs.

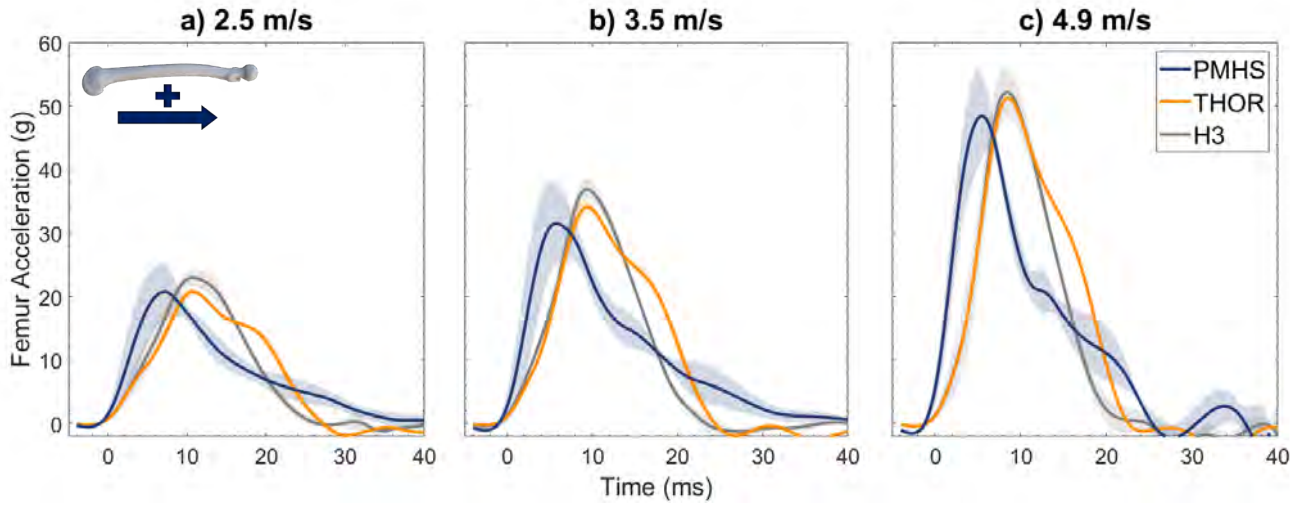

Fig. 5. Average femur acceleration in the A-P direction measured for PMHS, THOR, and Hybrid III (± one standard deviation) for impact velocities of a) 2.5 m/s, b) 3.5 m/s, and c) 4.9 m/s.

Femur Loading

Femur forces measured by the THOR-05F and Hybrid III ATDs were compared to the results obtained from the PMHS LPMs for each impact velocity (Fig. 6). The loading traces for the ATDs were again a closer match to each other than to the PMHS, although the Hybrid III exhibited two separate loading rates prior to the peak force, stiffening about halfway through and deviating from the THOR response. Similar to the force recorded at the knee, the Hybrid III ATD had the largest loading rate and maximum force, while also having the shortest time to

peak force and loading duration (Table E2). Further, the PMHS loading behaviour for the femur once again exhibited the opposite trends, with the smallest loading rate and maximum force, and the longest time to peak force and loading duration (Table E1). Impulses were also similar between subjects (Tables E1-E3).

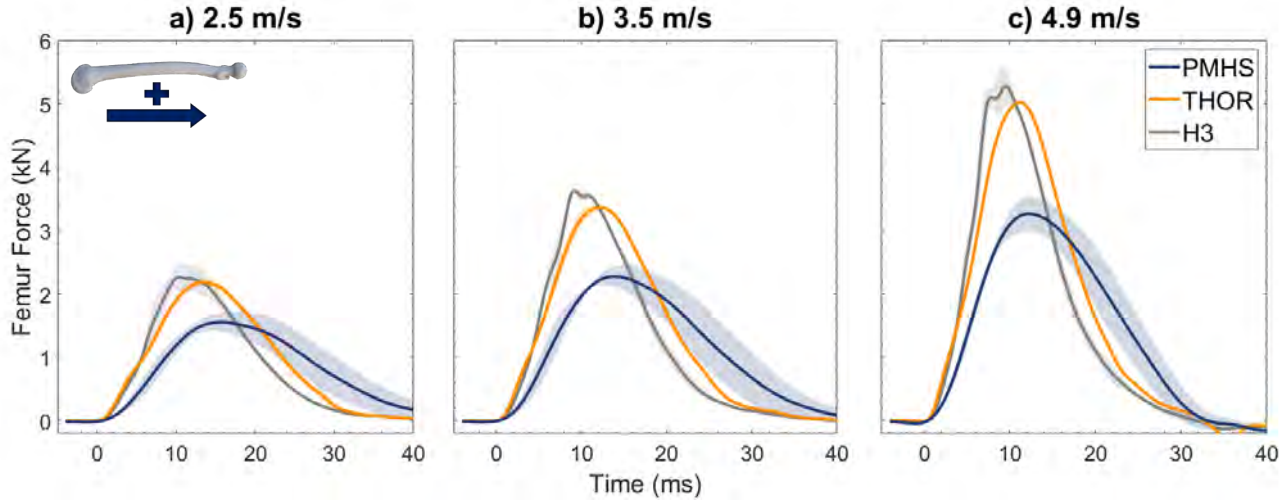

Fig. 6. Average femur force along the z-axis measured for THOR and Hybrid III (± one standard deviation) compared with average results predicted by the female PMHS LPM in [1] for impact velocities of a) 2.5 m/s, b) 3.5 m/s, and c) 4.9 m/s. Positive femur force is directed in the A-P direction.

Pelvis Kinematics

Pelvis acceleration-time histories are shown in Fig. 7, with A-P pelvis acceleration representing a positive value. Detailed pelvis translational and rotational kinematics for each subject can be found in Appendix F. While peak pelvis accelerations varied between subjects and impact velocities, the trends were consistent across tests. The Hybrid III ATD exhibited the highest average maximum acceleration across all impact velocities (31.6 ± 3.9 g for 2.5 m/s impacts, 59.2 ± 8.3 g for 3.5 m/s impacts, and 88.8 ± 1.1 g for 4.9 m/s impacts), characterized by an abrupt increase or spike occurring prior to 10 ms. The spike was absent in the response of the THOR ATD, which exhibited maximum accelerations of 25.2 ± 0.4 g for 2.5 m/s impacts, 39.5 ± 2.0 g for 3.5 m/s impacts, and 59.1 g for the 4.9 m/s impact. Lastly, while PMHS peak magnitudes were lower (24.4 ± 10.4 g for 2.5 m/s impacts, 36.0 ± 13.9 g for 3.5 m/s impacts, and 49.8 ± 15.3 g for 4.9 m/s impacts), the acceleration remained positive for a more sustained duration than for the ATDs and was more oscillatory in nature. The time to maximum pelvis acceleration during the initial peaks occurred within 7-11 ms following the impact for each subject and each impact velocity. These values, on average, represented a delay from the time to maximum femur acceleration for the PMHS and THOR tests, while the maximum pelvis acceleration occurred earlier in the Hybrid III tests.

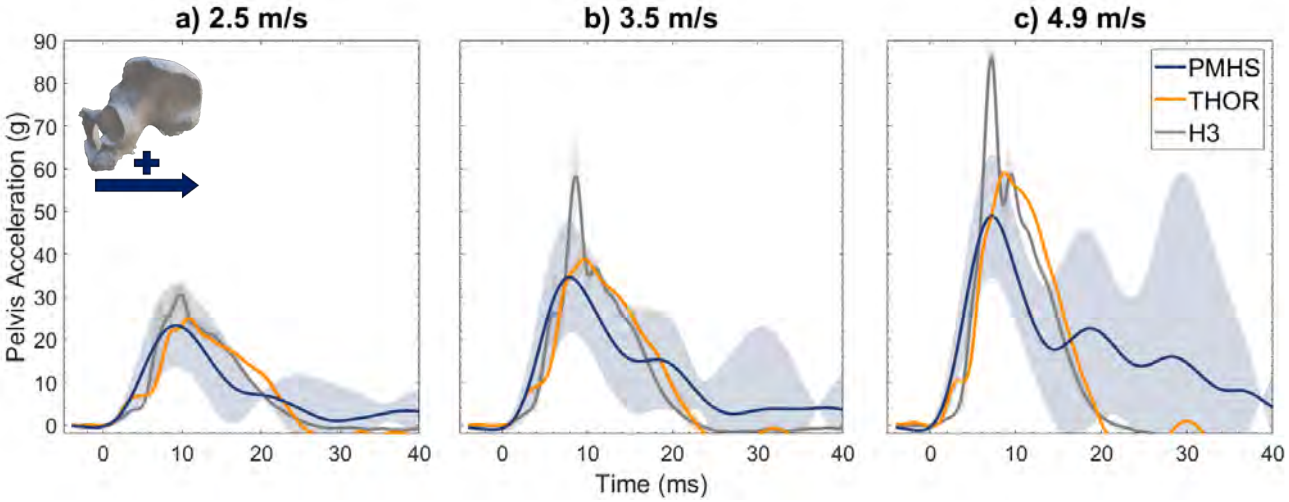

Fig. 7. Average pelvis x-axis acceleration in the A-P direction measured for PMHS, THOR, and Hybrid III (± one standard deviation) for impact velocities of a) 2.5 m/s, b) 3.5 m/s, and c) 4.9 m/s.

The PMHS displayed the largest forward and rearward pelvis angular motion across all tests, and the difference between the PMHS and ATD angular rates increased with increasing impact velocity (Fig. 8-9). Both

ATDs experienced only forward pelvis rotation as the impact at the hip drove the inferior portion of the pelvis rearward. For PMHS tests, the pelvis initially rotated rearward upon impact, but then switched to forward rotation after the time of peak force. The Hybrid III and THOR ATDs exhibited similar motion in the initial and final 10 ms of the testing window. Between 10 ms and 30 ms, the two ATD responses differ. In terms of angular displacement (Fig. 9), this results in a delay in the THOR response (23.0 ms for 2.5 m/s impacts, 15.8 ms for 3.5 m/s impacts, and 9.6 ms for 4.9 m/s impacts). When comparing the maximum angular displacements, the Hybrid III and THOR have similar peaks of 22.1 ± 0.6 deg and 24.6 ± 0.3 deg for 2.5 m/s impacts, 25.7 ± 0.8 deg and 24.9 ± 0.6 deg for 3.5 m/s impacts, and 28.4 ± 0.4 deg and 26.3 deg for 4.9 m/s impacts, respectively. Compared to the ATDs, the maximum angular displacements for the PMHS were greater with average values of 26.2 ± 4.7 deg, 31.3 ± 3.9 deg, and 37.7 ± 7.5 deg for each respective impact velocity, however the timing of these peaks were in between the timing of the ATDs. Finally, despite the differences in the maximum angular displacements, all subjects exhibited minimal pelvis angular displacement at the time of maximum applied knee force (-2.0 ± 1.8 deg for PMHS, 0.9 ± 0.1 deg for Hybrid III, and 0.5 ± 0.2 deg for THOR).

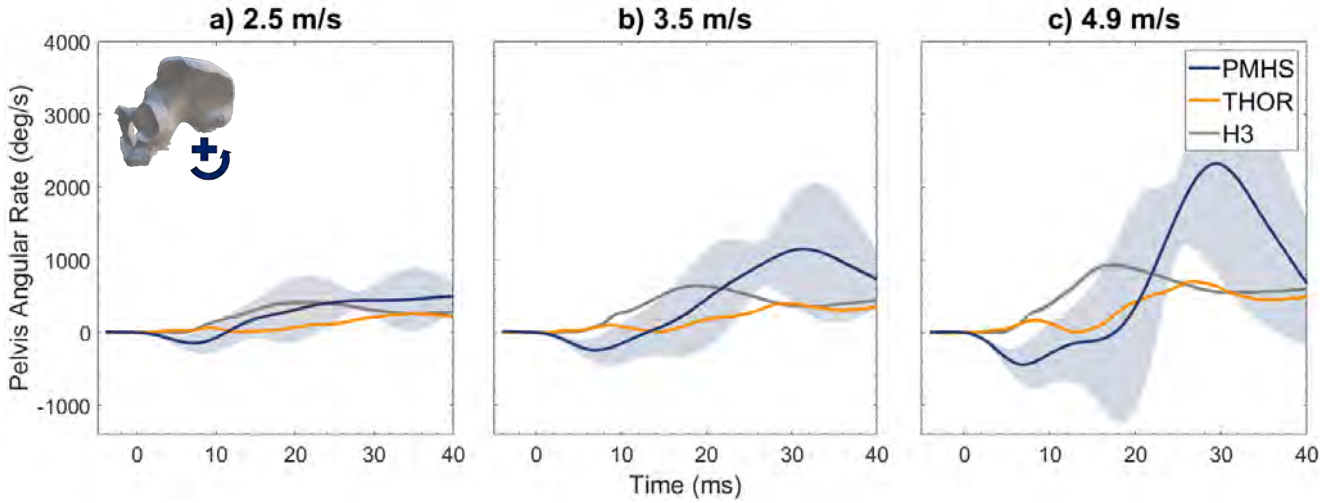

Fig. 8. Average pelvis angular rate about the y-axis measured for PMHS, THOR, and Hybrid III (± one standard deviation) for impact velocities of a) 2.5 m/s, b) 3.5 m/s, and c) 4.9 m/s. Forward pelvis rotation represents a positive value.

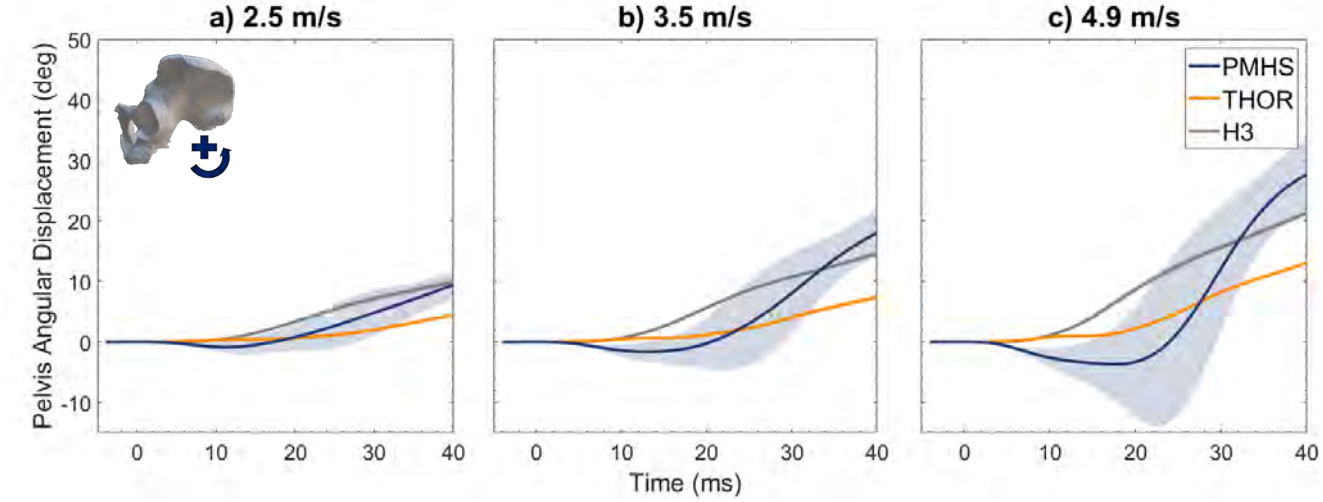

Fig. 9. Average pelvis angular displacement (in degrees) about the y-axis measured for PMHS, THOR, and Hybrid III (± one standard deviation) for impact velocities of a) 2.5 m/s, b) 3.5 m/s, and c) 4.9 m/s. Forward pelvis rotation represents a positive value.

Hip Loading

Hip forces measured in the THOR-05F and predicted using the Hybrid III LPM were compared to the results obtained from the PMHS LPMs for each impact velocity (Fig. 10). Hip loading characteristics were then calculated and analysed for trends between the different subjects at varying impact velocities (Appendix G). Loading behaviour followed similar trends to before, except for maximum force in which the THOR-05F had the smallest maximum force across all impact velocities. The initial loading rate of the THOR-05F matched the PMHS

more closely than the Hybrid III, but the post-maximum load reduction rates of the ATDs were nearer to each other than either was to the PMHS. This shift in behaviour results in less impulse transferred to the hip (40.4% of the initial impulse at the knee) for the THOR-50M compared to the other subjects (>60% transferred).

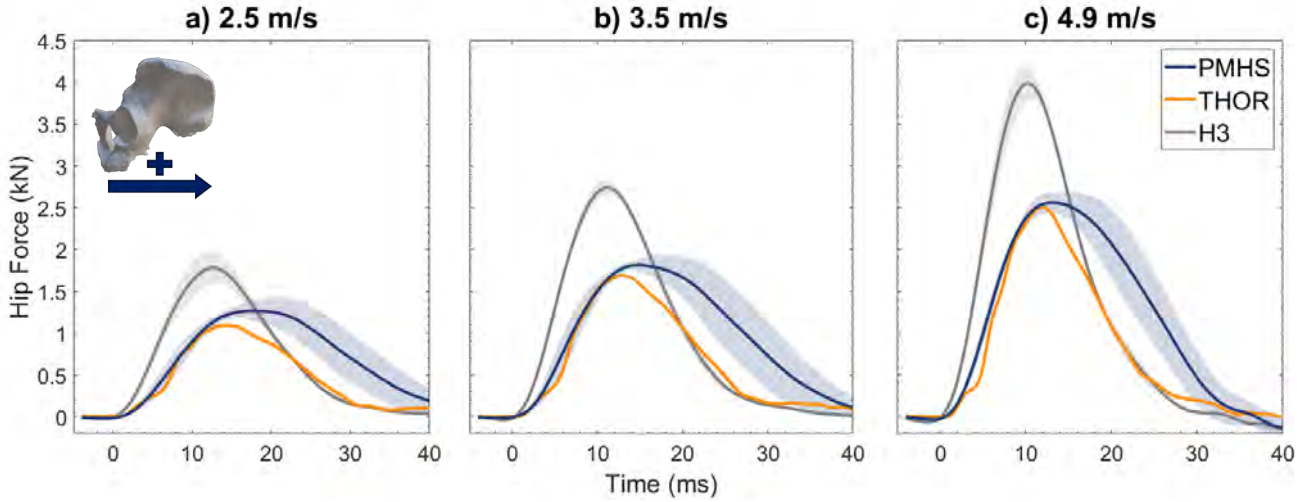

Fig. 10. Average hip force measured/predicted for PMHS, THOR, and Hybrid III (± one standard deviation) for impact velocities of a) 2.5 m/s, b) 3.5 m/s, and c) 4.9 m/s. Positive hip force is directed into the acetabulum, loading the pelvis in the A-P direction.

Force Transfer

Plots of the average traces for the knee, femur, and hip forces for the PMHS and the ATDs are shown for each impact velocity in Appendix H (Fig. H1-H3). Loading behaviour along the entirety of KTH was then analysed to determine the force drop predicted/measured from the knee to the femur and the hip in the ATDs. The results were then compared with the results of the PMHS LPMs. Results are reported both as the average percentage of force transferred for each subject ± one standard deviation (Fig. 11, Tables H1-H3), and as a scalar multiple of the PMHS forces (Table H4), where ratios greater than one indicate that the ATD measurement location is overpredicting the force in the PMHS. The resulting force transfer measured by the Hybrid III femur load cell was 79.4±2.4% of the initially applied force at the Hybrid III knee. Similarly, the resulting force transfer measured in the THOR femur load cell was 82.7±0.4% of the force applied to the THOR knee. Both percentages were higher than the PMHS which had a predicted force transfer of 70.6±1.7% from knee-to-femur. At the hip, the predicted knee-to-hip force transfer for the Hybrid III ATD (via the LPM) was 60.6±0.5%. For the THOR ATD, there was a larger drop in force between the femur load cell and acetabulum load cell as 41.4±0.4% of the initially applied force at the knee went into the hip. The PMHS knee-to-hip force transfer was most similar to the Hybrid III at 57.0±3.0%.

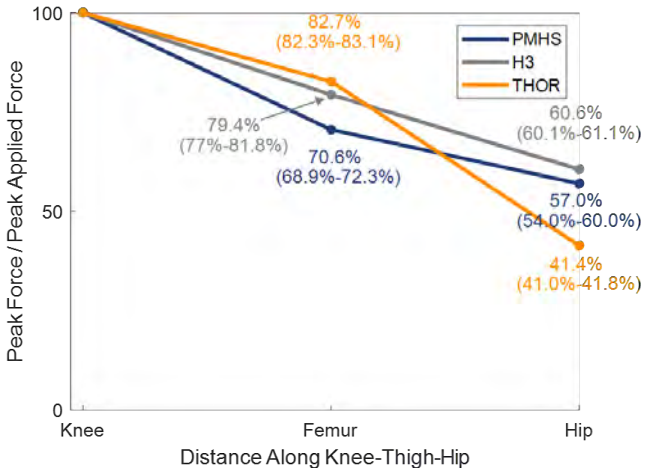

Fig. 11. Average knee-thigh-hip force transfer normalized for each subject (representing similar impact forces at the knee such as theorized through the use of force limiting bolsters by [6]).

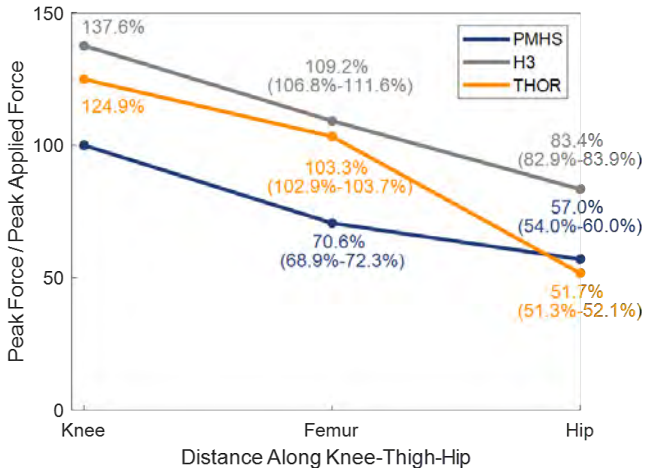

Fig. 12. Average knee-thigh-hip force transfer normalized as a percentage of the PMHS applied force (representing the relationship under the test-specific impact conditions).

As reported previously in [6], the only theoretical situation in which the initial force at the knees would be equivalent amongst subjects (the normalized graph in Figure 11), is in the presence of a force limiting bolster. Under such theoretical loading conditions, the ATD femur forces would overpredict the PMHS femur force by approximately 1.15 (1.12 for Hybrid III and 1.17 for THOR). At the hip, the Hybrid III would be a slightly overprediction (1.06), while THOR would underpredict by a factor of 0.73. Comparing the ATD force transfer responses by scaling them relative to the PMHS experimental data (Fig. 12), the ATD femur forces overpredicted the femur force in the PMHS by a factor of approximately 1.50 (1.55 for Hybrid III and 1.46 for THOR). For the hip, the Hybrid III overpredicted hip forces by a factor of 1.46, whereas THOR was closer in magnitude at 0.91 (slight underprediction).

IV. DISCUSSION

Hybrid III Lumped Parameter Model Validation

In the absence of load cells at the acetabulum in the Hybrid III ATD, whole body scaling techniques were used to adapt the original Hybrid III mid-size male LPM reported in [6] for use with the small female ATD. This approach was chosen as damage to the Hybrid III prevented the continuation of testing; thus, only the whole-body tests were used in this analysis. Appendix B lists the original model parameters along with the updated parameters used for the current testing. Figures B3-B5 show a comparison of the measured and predicted whole-body femur accelerations, femur forces, and pelvis accelerations at each of the different impact velocities tested. Predicted femur forces and accelerations aligned closely with the measured values at each of the impact velocities, and any differences between the two were comparable to the differences reported previously by [6] for the mid-size male tests. Model-predicted pelvis accelerations roughly captured the overall shape of the measured values throughout the test duration but failed to capture oscillatory spikes in the acceleration which consistently occurred prior to the peak force timing (Fig B5). Similar behaviour was also present in the mid-size male pelvis accelerations prior to the peak load, though the magnitude of these spikes were lower than those observed in the present study. It is unknown currently why this occurred across both test series. One possible explanation is that the behaviour is related to the force along KTH overcoming the stiffness of the coupling with the ATD torso to allow it to rotate forward during the impact. Further, while it was not specifically discussed in the previous study, in situations where the Hybrid III was tested under similar conditions with the torso removed, there is an observable decrease in the magnitude of these oscillations. In terms of understanding and assessing the validity of the results from the Hybrid III LPM reported in this study, the model may not capture the oscillatory peaks in pelvis acceleration but appears to capture the average of the oscillations. This indicates that the impulse of loading calculations should remain valid as there are cases when the impulse is overpredicting and cases when it is underpredicting. Similarly, the presence of the oscillations suggests that there are periods where the hip loading rate is both greater and less than the reported value. This would also theoretically equate to the average predicted by the model. Lastly, the predicted pelvis acceleration beyond the peak knee force is consistent with the measured value. This suggests that the maximum hip force and overall force transfer results are also still valid since these measurements are independent of the oscillations occurring prior to the peak force; the increased pelvis acceleration from the oscillatory spikes would result in less of a reaction force built up behind the hip while the force is delivered at the knees. Thus, while oscillatory behaviour is present in the pelvis accelerations prior to the peak knee force, it should not affect the hip force results obtained from the model.

Variations in Impact Force

For the same impact conditions at the knee, the ATD forces and loading rates were higher than the PMHS forces. This behaviour is consistent with past studies studying knee impact forces in mid-sized males, where it was determined that the forces anywhere in the Hybrid III KTH complex would be different from the corresponding locations in the PMHS [6-8]. Additionally, [6] showed that this behaviour depended on the impactor design. For impactor materials which are not force limiting, the resulting forces will depend on the amount of deformation of the material. For subjects with similar masses, the stiffer subject will have greater effective mass, and thus will result in larger impactor deformations and a higher force. The material used in the present study was not force-limiting; since the ATDs had higher knee impact forces and loading rates, it follows that the ATDs were stiffer than the PMHS. This agrees with previous findings for other regions of the ATDs under varying load conditions [9,10].

Variations in Mass Recruitment Up to the Time of Maximum Hip Force

The means of mass recruitment along KTH differed between the PMHS and the ATDs. The Hybrid III ATD had greater coupling (i.e., higher stiffness and damping) between its masses than the PMHS (Tables A1 and B1). Thus, when the system was impacted, the force was transferred immediately throughout KTH, and all the masses were recruited simultaneously (Fig. H1-H3). A similar trend was seen in previous KTH tests on the Hybrid III 50th percentile male ATD [6]. The THOR-05F behaved like the Hybrid III in force transfer from the knee to the femur, but not in force transfer from the femur to the hip. Similarities with the PMHS during the loading period up to the peak force are likely attributable to the design of the THOR-05F femur which includes an axially compliant bushing between the femur load cell and the acetabulum. This design permitted the magnitude of hip force in the THOR-05F to better match the PMHS response by providing a means of energy dissipation during femur compression, as intended in the biomechanical response targets [11].

Variations in Force Transfer Relationship with Impact Boundary Conditions

The force transfer relationship between ATDs and PMHS has been shown to depend on the impact boundary condition [6]. In the case of automotive restraint design, knee bolsters with arbitrary nonlinear stiffness invalidate the assumption of a singular, unique relationship between ATD and PMHS response. For the THOR-05F, this challenge is further complicated by its force transfer behaviour (Fig. 11). Due to the complexity of varying knee impact conditions, it becomes challenging to derive one singular relationship between the force transfer in the ATDs and the PMHS (Table H4). A previous investigation by [6] showed that these values can be bounded by a lower force limit and an upper force limit comparison. While the impact conditions in the study did not use a force-limiting bolster, the force-limiting bolster impact, specifically the condition where the subjects are at or exceed the force limit (thus the applied forces are equivalent across subjects), theoretically produces the lowest force limit of comparison between subjects. For mid-sized male PMHS and ATDs impacted under these conditions, the PMHS hip forces were estimated to be about 1.3 times higher than the THOR-NT [12], whereas the Hybrid III hip force was predicted as slightly higher than the PMHS [6]. The trends for female subjects under these conditions are similar to the males (Fig. 11). For a predicted PMHS force at the hip, the Hybrid III femur force would be about 1.39 times greater (79.4%/57.0%), whereas the hip force would be approximately 1.06 times greater (60.6%/57.0%). For THOR, the femur force would be approximately 1.45 times greater than a given PMHS hip force (82.7%/57.0%), however the THOR hip force would be lower than the PMHS by a factor of 1.38 (57.0%/41.4%). Unlike the lower force limit, the upper force limit requires a more in-depth analysis incorporating a range of knee-bolster designs observed in motor vehicles. While the bolster used in this testing represents just one impact condition where the knee forces differ between subjects, future work should assess the response to impacts with knee bolsters of varying design, similar to what was done in [6].

Comparison to Biomechanical Response Target

Fig. 13 depicts the hip force measured in the THOR ATD compared with the estimated female PMHS hip force, and the hip force obtained via scaling the estimated PMHS mid-sized male hip force [3] by the recommended factor of 0.79 from [11]. Fig. 14 shows the same three plots but introduces a time scaling factor of 0.86 for the mid-sized male data yielding the biomechanical response target established for the THOR-05F. While maximum force was similar to the female subjects when only scaling the predicted PMHS mid-sized male hip force in magnitude (Fig. 13), introducing a time scaling factor produced a response which peaked earlier than what was observed for the PMHS and THOR hip forces (Fig. 14). In addition to similar maximum forces between the scaled values and the female PMHS and THOR-05F, the scaled loading rates across both impact velocities were also the same. This suggests that both the maximum force and initial loading rates for the female PMHS can be reasonably approximated by scaling the male PMHS data, and that the THOR-05F is able to capture this behaviour under the current test conditions. Although the KTH response in the THOR-05F is consistent with the scaled male data and the female PMHS response up until the maximum force, the behaviour after the maximum force tells a different story. The THOR-05F hip force decreases immediately and has a smaller impulse than the female PMHS and scaled male PMHS. Additionally, the impulse of loading in the female PMHS is greater than the scaled male results. This suggests that there may be an additional factor that is causing a variance in the behaviour after the peak force.

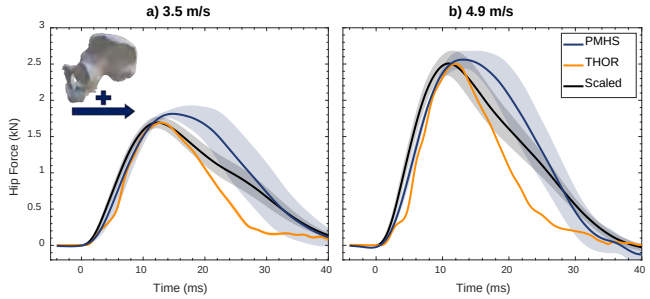

Fig. 13. Average hip force estimated for female PMHS and measured for THOR compared to the hip force predicted by simulating the mid-sized male whole body KTH tests in the NHTSA Biomechanics Database (for equivalent conditions) with the LPM from [3] and scaling only the force value for a small female according to [11].

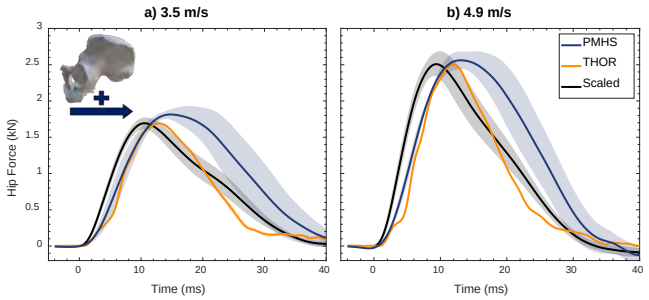

Fig. 14. Average hip force estimated for female PMHS and measured for THOR compared to the hip force predicted by simulating the mid-sized male whole body KTH tests in the NHTSA Biomechanics Database (for equivalent conditions) with the LPM from [3] and scaling the force and time values for a small female according to [11].

Potential Influence of Pelvis-Sacrum-Lumbar Spine Kinematic Interaction

While this study utilizes current tools in the field (analytical models and ATDs) for estimating the kinematic behaviour and force transfer along KTH in female PMHS, the tools were ultimately unable capture every aspect of the KTH impact observed in the PMHS. Further, although this comparison is a useful starting point, the ultimate concern as researchers in the field of injury biomechanics is how we can use these results to predict (and reduce) injury risk. To fully address this concern, it then becomes crucial to understand the applicability of the approaches and the message that these approaches convey in the context of the current injury patterns observed in the field data. Recall that in an epidemiology study by [4], the authors determined that females were 1.89 times more likely to sustain an injury to KTH, even after controlling for relevant crash characteristics, and the cause of this difference in risk remains unknown. Similar conclusions were also drawn by [5] in a later investigation. Because the implications of the increased odds ratios are not something that should be taken lightly, it becomes critical to consider alternate factors that may contribute to the injury patterns, especially when it appears that employing mass scaling can account for most of the initial force behaviour at the hip, and certainly doesn't spotlight any immediate areas of concern.

Due to the simplified testing environment, the observations that the PMHS and ATDs displayed differences in pelvis kinematics as well as variations in hip force after the peak force provides one avenue for further investigation. For the same impact conditions at the knee, the PMHS exhibited greater rotational motion at the pelvis. Further, the difference in angular displacement between the PMHS and ATDs increased with increasing impact velocities. The explanation provided previously when analysing the force transfer in a KTH impact for mid-sized males is that the magnitude of pelvis rotation during knee impact loading under a free back condition is largely dictated by the inertia of the upper body holding the superior portion of the pelvis while the inferior portion translates rearward [3,6,13]. In knee impact tests without the upper body, this absence resulted in the pelvis rotating in an opposite direction than observed in all other test conditions. In the context of the experimental data in this test series, forward pelvis rotation may be dependent on not only the presence of pelvis coupling to the upper body, but also how the pelvis couples and when this interaction occurs.

For the PMHS response after the maximum hip force, the response appears to be dictated by increased coupling of the upper body at a later time frame than observed with the ATDs. In the original experimental work performed using the female PMHS, pelvis kinematics were tracked using a six degree-of-freedom sensor attached to the pelvis via a mount with threaded rods inserted into the left and right posterior superior iliac spine (PSIS)[1]. It is therefore possible that differences in these measurements come from experimental noise, although mount stability was tracked throughout testing to avoid testing in scenarios where the mount integrity was compromised. Another possibility is that the mobility (or laxity) of the articulating joints of the pelvis-sacrum-lumbar spine structure (hip, sacroiliac, and sacrococcygeal) play a much larger role in dispersing the energy of the KTH response for female subjects than the ATDs. Specifically, the hypothesis is that joint mobility presents itself during a KTH impact by placing the pelvis-sacrum-lumbar spine complex in a state of pelvic nutation where the relative rotation of the system forms a more favourable structure for bearing a mechanical

load (Fig. 15A). Here the pelvis moves posteriorly and inferiorly rotating about the sacroiliac joint (SIJ) while the load is applied. The response would then be followed by subsequent counternutation of the pelvis where the sacrum moves posteriorly and superiorly and rotates the pelvis in the opposite direction from a reverse moment about SIJ (Fig. 15B). The SIJ in females is known to be more mobile than that in males throughout aging, with a notable peak observed in younger females and even more pronounced during pregnancy [14-16]. This idea is supported by many years of previous research investigating the role of the SIJ in pelvic girdle and lower back pain, and the significance of the sacrum as a mechanical stabilizer during locomotion [14-30]. It has also been shown that lumbar flattening and lordosing are largely initiated by external motion of the pelvis on the hip joints [15,22,31]. Further, the effect of SIJ nutation is smaller with flattening of the lumbar spine, whereas this behaviour is more pronounced in a lordotic state [15,17,26-30]. Lastly, a recent study investigating changes in skeletal positioning in both young and elderly volunteers imaged in standing and seated postures found that females exhibited significantly higher changes in their pelvic tilt and sacral slope angle when transitioning from standing to sitting compared to the male cohort [32]. Since this is currently just a theory, further research will need to be performed investigating the feasibility of this mechanism; however, it is still critical when investigating reoccurring sex-based injury disparity patterns in the lower extremity region to continuously question the injury mechanisms involved.

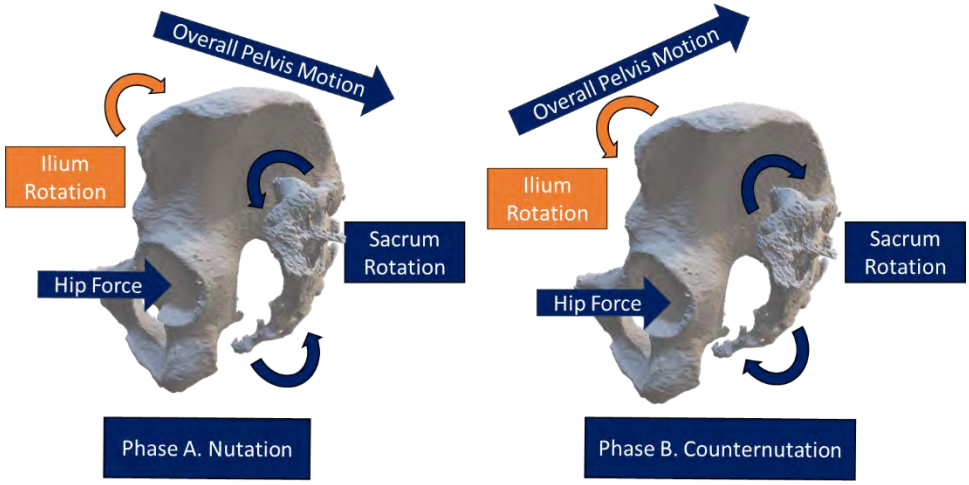

Fig. 15. Hypothesized mechanism for varying behaviour after the maximum force in females split into phase A) where mobility of the sacrum about the SIJ causing negative pelvis pitch with little involvement of the upper body (nutation), B) Reverse sacrum/ilium rotation followed by the inertial recruitment of the upper body over leading to the subsequent mechanism for pelvis rotation in males.

The significance of this coupling behaviour could also explain why, despite similar femur compression behaviour between the THOR and PMHS, the increased stiffness of the lumbar spine (and larger immediate mass coupling of the torso) lead to a drop in THOR hip force which follows well with the drop in force predicted at the Hybrid III hip (Fig. 10). Further, across all PMHS, there were variable oscillatory peaks in the pelvis acceleration response beyond the initial stages of the impact (after approximately 15 ms post impact), and this behaviour was not observed in the ATDs. This is all to say that improving the biofidelity of the ATD femurs in axial compression may only be capturing part of the KTH impact response, and further understanding the mechanical behaviour behind the hip might account for differences observed across prediction methods.

Other Factors Not Explored That Could Alter the KTH Impact Behaviour

While the influence of the pelvis-sacrum-lumbar spine kinematic interaction on the KTH response presents an intriguing avenue for future research, it is also important to acknowledge additional known factors that could alter the KTH impact response and were not explored in the current research. One study looked at how hip fractures occur from frontal crash scenarios and found that the angle of presentation of the acetabulum during these impacts as well as the size and shape of the femoral head and posterior acetabular wall were important in understanding the injury mechanism [33]. In cases where the acetabulum is oriented in line with the axial force transmitted from the impact at the knee, there was maximal surface area to distribute the load. Due to the increased surface area, an injury to the knee or thigh was more likely to occur before injuring the hip. Another extreme scenario was noted from subjects whose acetabulum was directed laterally, leaving only the posterior

wall of the acetabulum to absorb the load. In this scenario, dislocations of the femur from the hip and posterior wall fractures are more likely to occur due to the decreased surface coverage. The authors also found that seated males typically had an acetabulum directed more horizontally and laterally, a smaller average acetabular depth, and larger femoral heads compared to the females. This would seemingly contradict the findings from the field data, as it suggests that the female hip should be more stable to loading from an axial force applied at the knees and should be explored in future work.

Hip positioning at the time of impact has also been identified in multiple studies as a potential contributor to variation in the KTH response, and a similar narrative was provided for acetabular presentation [34-37]. When hip posture deviated from a neutral posture, hip tolerance decreased by an average of 34±4% with 30 degrees of hip flexion (significant, $p<0.0001$), and by 18±8% with 10 degrees of hip adduction (significant, $p=0.008$) [34]. This decrease in tolerance comes from decreasing surface coverage between the femur and acetabulum, resulting in greater localized stresses. Further, it was reported in [37] via correspondence that there was a 0.6% decrease in load-bearing area per degree of flexion from a standard driving posture and 0.9% increase in load bearing area per degree of adduction from a standard driving posture. In testing performed by [37], the authors reported similar findings. In a study investigating sex-based differences in preferred seating postures by [38], males in the studies typically assumed a more slouched posture against the seatback with more posterior rotation of the pelvis and a more diffuse pressure profile. In contrast, females typically sat closer to the front of the seat with less slouching, had a more focal seat pan pressure profile, and exhibited greater anterior rotation of the pelvis. In the context of occupant positioning, the more anteriorly rotated pelvis in the female volunteers would likely result in greater hip flexion and theoretically place the female occupants in a less ideal position for receiving a load at the hip [34,37]. It is important to mention that this study focused on the sagittal view, although there is a notion that females sit in vehicles with less leg splay (hip abduction) compared to males. Such behaviour would also place female occupants in less ideal positioning for dispersing a load at the hip, although this notion appears more anecdotal at the current time. Future studies looking at naturalistic driving postures should seek to investigate this notion further.

A final potential factor that was not explored in the current work is the effect of muscle activation stemming from pre-impact bracing manoeuvres. In a previous modelling study, it was observed that muscle activation increased the mass coupling directly between the impact at the knee to the hip, resulting in a lower percentage of force transferred to the hip. Because of this, the studies both concluded that the presence of muscle tension decreased the force at the knee required to cause KTH fracture, as more energy from a given impact would be absorbed immediately along KTH. In [39], the authors saw an increase in the likelihood of femoral shaft fractures by 20%-40% with muscle activation, but also noted that this behaviour had little effect on the likelihood of hip fractures. These findings were also supported by another modelling study looking at the effects of muscle activation, where it was shown that bracing increased the peak axial femur force by 45.8% compared to the relaxed condition [40]. In addition to increasing femur force, it was also observed that muscle activation increased the bending moments in the femoral shaft due to the curvature of the femur in the medial-lateral direction. This is all to say that pre-impact bracing manoeuvres performed prior to a motor vehicle collision would also affect the force transfer comparison between humans and ATDs, altering our ability to predict these injuries through ATD tests. Finally, although unknown at the current time, if sex-based differences in pre-impact bracing manoeuvres exist, this could also contribute to the injury patterns in the field data.

Limitations

The results from this study are an important first step in understanding the applicability of the current small female ATDs for simulating the KTH response. To the authors' knowledge, this is the first study to compare the force transfer along KTH of small female ATDs with female PMHS tested under similar conditions, providing a preliminary comparison aimed towards reducing the sex-based injury odds disparities in the field data. With that, it is still important to address key limitations with the current findings.

First, the goal of this testing was to compare the KTH impact response of female PMHS with small female ATDs in simplified test conditions. Subjects were bilaterally impacted at the knees in an upright free-back condition, with the inertial response of the system dictated by a ram. This setup removes many complexities introduced by a vehicle environment, allowing for a comparison of the KTH impact behaviour at a more fundamental level. While any of the differences observed in the current study might be present to some degree in a frontal motor vehicle collision, the simplified nature of the current setup is unable to capture all aspects of

a frontal collision. As mentioned previously, there are other factors that weren't explored that may alter the findings, including differences in physiological factors such as the angle of presentation of the acetabulum or social factors such as occupant posture and distance to the lower instrument panel at the time of impact, occupant bracing status, or seat belt usage (including if the belt was properly worn). It is important to note that the results of this study do not preclude other factors from altering the response, and it is intended that more complexity will be introduced into the analysis with follow-up work. Additionally, positioning of the occupants for this test series are based on the Hybrid III mid-sized male's positioning when the knees strike the lower instrument panel, which may or may not be applicable for female occupants [3]. The fundamental mechanical principles of inertial losses would still apply, reiterating the utility of this simplified experimental approach; however, differences in the pre-impact positioning would alter the initial mass coupling state of the occupant. Lastly, as discussed in previous work, asymmetrical impacts have the potential to favour increased hip loading on the side with greater knee force due to an uneven buildup of mass, which would otherwise be absent in a symmetric impact, and further affect the ability to determine a force transfer relationship across subjects [6]. Further, the presence of asymmetrical impacts would suggest a torsional component about the z-axis of the pelvis and upper body that is not captured by the current LPM. While the extent of this warrants further investigation, it would be theoretically be affected by factors such as pelvis geometry, with a wider pelvis resulting in a larger torsional moment, and joint mobility, both of which representing areas of sexual dimorphism.

Second, all kinematic measurements compared in the present study were measured from sensors directly mounted to the subjects throughout testing, while the PMHS femur and hip force as well as Hybrid III hip force were predicted model-based measures used for comparisons. While the one-dimensional LPM used to compare KTH force transfer in the absence of load cell data represents the currently established methodology for comparing this response, the results cannot be completely validated at this time without installing acetabular load cells inside the PMHS or Hybrid III and are limited to symmetric knee loading. Additionally, even with the ability to capture the hip force in the PMHS, the installation of these sensors would likely compromise the mass coupling along KTH prior to testing. Therefore, as more capabilities become available for evaluating and comparing the KTH impact response across subjects, these models may need to be reevaluated. Future studies should also analyse the performance of the female models presented in various loading cases to understand the extent of their applicability.

Third, the occupants were compared using one impactor material. A previous methodology has been reported using theoretical investigations of this behaviour across a range of characteristic knee impacts [6]. Here, it was observed that the KTH force transfer relationship between PMHS and ATDs are not singular, and instead the force transfer relationship is highly sensitive to the parameters of the impacting material. While the authors intend to investigate this relationship in future work as it pertains to the female PMHS, the lack of a singular relationship across subjects is indicative that a singular Injury Assessment Reference Value (IARV) based on load cells in the femur or acetabulum of the ATDs is likely not suitable across the range of bolster designs observed in motor vehicles. Further, introducing variability in mass coupling and recruitment behaviour enhanced due to the various factors discussed may not only substantially alter the pre-impact positioning and the resulting kinematics, but also the force transfer relationship across subjects. Even with relationships established, these values are based on models, and thus subject to change as more capabilities become available, or if the behaviour deviates in other loading conditions.

Finally, the four female subjects tested in the original study were between 46-70 years old. Females experience unique physiological changes throughout the aging process, and it is unclear at this time the extent to which the four subjects were able to represent this behaviour. Further, recent epidemiology studies have shown that the injury disparity present in the field data trends towards younger females, contradicting the notion that this behaviour is purely a result of post-menopausal factors [4,5]. Since this demographic is underrepresented in biomechanics testing, this limitation is not unique to the current study and spotlights an ongoing issue that injury biomechanics researchers face while attempting to understand the continuation of the lower extremity injury disparity. This disparity is also not limited to frontal motor vehicle collisions and has also arisen in sports [41], military [42], and space [43] applications. Acknowledging this, some potential avenues for future research include exploring physiological differences in joint mobility across age and sex, or naturalistic driving studies to discern if the patterns stem from variations in occupant behaviour while interacting with the

vehicle environment. Despite this and the previously mentioned limitations, the results still appear promising for future investigation of the sex-based KTH injury disparity observed in frontal motor vehicle collisions and provides areas for potential biofidelity improvements in the ATDs.

V. CONCLUSIONS

This study analysed the loading and kinematic responses of 5th-percentile female ATDs in a bilateral knee-impact test condition. Results were then compared to small female PMHS tests and LPMs that were derived in a previous study. In general, the Hybrid III ATD had the largest loading rate and maximum force, and the smallest loading duration and time to peak force for each point along KTH. Conversely, the PMHS generally had the smallest loading rate and maximum force, and the largest loading duration and time to peak force for each point along KTH. The force transfer from the knee to the femur was 79.4 ± 2.4% for the Hybrid III 5th percentile female, 82.7 ± 0.4% for the THOR-05F, and 70.6 ± 1.7% for the PMHS. The force transfer from the knee to the hip was 60.6 ± 0.5% for the Hybrid III 5th percentile female, 41.4 ± 0.4% for the THOR-05F, and 57.0 ± 3.0% for the PMHS. Thus, for the impact conditions tested in this study, the Hybrid III femur force was approximately 1.92 times greater than the force predicted at the PMHS hip, and the predicted Hybrid III hip force is approximately 1.46 times greater. For the THOR ATD, the femur force measured was approximately 1.81 times greater than the predicted force at the PMHS hip, however the hip force was a slight underprediction at 0.91. Variation in the force transfer relationship suggests a single IARV based on load cell measurements in the ATDs is likely not suitable across the range of bolster designs observed in motor vehicles. Finally, although maximum force at the hip is a helpful parameter in understanding KTH force transfer, none of the prediction tools evaluated appear to sufficiently describe the oscillatory pelvis kinematics in a simplified setup. While it is certainly reasonable that this could also be attributed to experimental noise, the force transfer behaviour in this study alone does not appear to be a sufficient explanation for the injury disparity observed in the field data, as it appears that a large portion of the KTH force transfer behaviour can be accounted for through simple scaling methods. Alternate explanations for this were provided, as were limitations to the current analysis, and suggest that increased attention may need to be placed on understanding sex-based differences in lower extremity seating postures and pre-impact bracing manoeuvres in the automotive setting, as these factors have been previously observed to alter KTH force transfer behaviour and would subsequently alter the capabilities of ATDs to reliably predict the force transfer behaviour. The effect of increased mobility in the articulating joints of the pelvis-sacrum-lumbar spine structure was also considered, as this mobility is a unique consideration for females throughout the aging process and would theoretically alter the mass coupling capabilities in this region, but the magnitude of this effect is unknown at the current time.

VI. ACKNOWLEDGEMENT

The following research was funded by the National Highway Traffic Safety Administration (NHTSA) under contract number DTNH2215D00022. The authors would also like to thank the staff at the University of Virginia's Center for Applied Biomechanics for all their help in this test series.

VII. REFERENCES

[1] Carpenter RL, Berthelson PR, Donlon JP, and Forman JL. Quantifying Female Subject-specific Knee-thigh-hip Responses in Frontal Impact Scenarios, in *Proceedings of the International Research Council on the Biomechanics of Impact (IRCOBI)*. 2023: Cambridge, United Kingdom. p. 978-1012.

[2] Sochor M and Rupp J. Commentary: Emergency Department Patients and Crash Test Dummies: What Do They Have in Common? *Annals of Emergency Medicine*, 2005. 46(2): p. 169-171

[3] Rupp JD, Miller CS, et al. Characterization of knee-thigh-hip response in frontal impacts using biomechanical testing and computational simulations. *Stapp Car Crash J*, 2008. 52: p. 421-74

[4] Forman J, Poplin GS, et al. Automobile injury trends in the contemporary fleet: Belted occupants in frontal collisions. *Traffic Inj Prev*, 2019. 20(6): p. 607-612

[5] Brumbelow ML and Jermakian JS. Injury risks and crashworthiness benefits for females and males: Which differences are physiological? *Traffic Inj Prev*, 2022. 23(1): p. 11-16

[6] Rupp JD, Reed MP, Miller CS, Madura NH, and Klinich KD. Development of New Criteria for Assessing the Risk of KTH Injury in Frontal Impacts Using Hybrid III Femur Force Measurements, in *Proceedings of the 21st (ESV) International Technical Conference on the Enhanced Safety of Vehicles*. 2009, National Highway Traffic Safety Administration: Stuttgart, Germany.

[7] Donnelly BR and Roberts DP. Comparison of Cadaver and Hybrid III Dummy Response to Axial Impacts of the Femur. *Stapp Car Crash J*, 1987. 31: p. 12
[8] Masson C and Cavellero C. Comparison between Hybrid III Dummy and Cadaver knee response in frontal impact. *Proceedings of Proceedings of the International Conference on the Biomechanics of Impact (IRCOBI)*, 2003. Lisbon, Portugal
[9] Parent D, Craig M, and Moorhouse K. Biofidelity Evaluation of the THOR and Hybrid III 50(th) Percentile Male Frontal Impact Anthropomorphic Test Devices. *Stapp Car Crash J*, 2017. 61: p. 227-276
[10] Wang JZ, Lee E, et al. Biofidelity Evaluation of THOR 5th Percentile Female ATD, in *Proceedings of the International Research Council on the Biomechanics of Impact (IRCOBI)*. 2018: Athens, Greece. p. 567-592.
[11] Lee EL, Parent DP, Craig MJ, McFadden J, and Moorhouse K. Biomechanical Response Requirements Manual: THOR 5th Percentile Female NHTSA Advanced Frontal Dummy. 2017, U.S. Department of Transportation. p. 54.
[12] Martin PG and Scarboro M. THOR-NT: Hip Injury Potential in Narrow Offset and Oblique Frontal Crashes, in *22nd International Technical Conference on the Enhanced Safety of Vehicles (ESV)*. 2011: Washington D.C. p. 16.
[13] Chang CY, Rupp JD, Kikuchi N, and Schneider LW. Development of a finite element model to study the effects of muscle forces on knee-thigh-hip injuries in frontal crashes. *Stapp Car Crash J*, 2008. 52: p. 475-504
[14] Brooke R. The Sacro-Iliac Joint. *J Anat*, 1924. 58(Pt 4): p. 299-305
[15] Vleeming A, Schuenke MD, et al. The sacroiliac joint: an overview of its anatomy, function and potential clinical implications. *J Anat*, 2012. 221(6): p. 537-67
[16] Kiapour A, Joukar A, et al. Biomechanics of the Sacroiliac Joint: Anatomy, Function, Biomechanics, Sexual Dimorphism, and Causes of Pain. *Int J Spine Surg*, 2020. 14(Suppl 1): p. 3-13
[17] Weisl H. The movements of the sacroiliac joint. *Acta Anat (Basel)*, 1955. 23(1): p. 80-91
[18] Joukar A, Shah A, et al. Sex Specific Sacroiliac Joint Biomechanics During Standing Upright: A Finite Element Study. *Spine (Phila Pa 1976)*, 2018. 43(18): p. E1053-E1060
[19] Kiapour A, Abdelgawad AA, et al. Relationship between limb length discrepancy and load distribution across the sacroiliac joint--a finite element study. *J Orthop Res*, 2012. 30(10): p. 1577-80
[20] Cusí M, Saunders J, Van der Wall H, and Fogelman I. Metabolic disturbances identified by SPECT-CT in patients with a clinical diagnosis of sacroiliac joint incompetence. *European Spine Journal*, 2013: p. 1674-1682
[21] Li J, Li Y, et al. Biomechanical analysis of sacroiliac joint motion following oblique-pulling manipulation with or without pubic symphysis injury. *Front Bioeng Biotechnol*, 2022. 10: p. 960090
[22] Vleeming A and Stoeckart R, "CHAPTER 8 – The role of the pelvic girdle in coupling the spine and the legs: a clinical–anatomical perspective on pelvic stability". 2007.
[23] Duncan M. The Behaviour of the Pelvic Articulations in the Mechanism of Parturition. *Edinb Med Surg J*, 1854. 81(201): p. 799-800
[24] Eichenseer PH, Sybert DR, and Cotton JR. A finite element analysis of sacroiliac joint ligaments in response to different loading conditions. *Spine (Phila Pa 1976)*, 2011. 36(22): p. E1446-52
[25] Hammer N, Steinke H, et al. Ligamentous influence in pelvic load distribution. *Spine J*, 2013. 13(10): p. 1321-30
[26] Vleeming A, Van Wingerden JP, et al. Mobility in the sacroiliac joints in the elderly: a kinematic and radiological study. *Clin Biomech (Bristol, Avon)*, 1992. 7(3): p. 170-6
[27] Sturesson B, Selvik G, and Uden A. Movements of the sacroiliac joints. A roentgen stereophotogrammetric analysis. *Spine (Phila Pa 1976)*, 1989. 14(2): p. 162-5
[28] Walheim GG. Stabilization of the pelvis with the Hoffmann frame. An aid in diagnosing pelvic instability. *Acta Orthop Scand*, 1984. 55(3): p. 319-24
[29] Lavignolle B, Vital JM, et al. An approach to the functional anatomy of the sacroiliac joints in vivo. *Anat Clin*, 1983. 5(3): p. 169-76
[30] Egund N, Olsson TH, Schmid H, and Selvik G. Movements in the sacroiliac joints demonstrated with roentgen stereophotogrammetry. *Acta Radiol Diagn (Stockh)*, 1978. 19(5): p. 833-46
[31] Boulay C, Tardieu C, et al. Sagittal alignment of spine and pelvis regulated by pelvic incidence: standard values and prediction of lordosis. *Eur Spine J*, 2006. 15(4): p. 415-22
[32] Mizukoshi R, Yagi M, et al. Gender differences in spinal mobility during postural changes: a detailed analysis using upright CT. *Sci Rep*, 2024. 14(1): p. 9154
[33] Wang SC, Brede C, et al. Gender differences in hip anatomy: possible implications for injury tolerance in frontal collisions. *Annual proceedings. Association for the Advancement of Automotive Medicine*, 2004. 48: p. 287-301
[34] Rupp JD, Reed MP, Jeffreys TA, and Schneider LW. Effects of hip posture on the frontal impact tolerance of the human hip joint. *Stapp Car Crash J*, 2003. 47: p. 21-33
[35] Rupp JD, Flannagan CA, and Kuppa SM. Injury risk curves for the skeletal knee-thigh-hip complex for knee-impact loading. *Accident Analysis and Prevention*, 2010. 42(1): p. 153-8
[36] Rupp JD, Flannagan CA, and Kuppa SM. An injury risk curve for the hip for use in frontal impact crash testing. *J Biomech*, 2010. 43(3): p. 527-31
[37] Salzar RS, Bass CR, et al. Development of injury criteria for pelvic fracture in frontal crashes. *Traffic Inj Prev*, 2006. 7(3): p. 299-305
[38] Dunk NM and Callaghan JP. Gender-based differences in postural responses to seated exposures. *Clin Biomech (Bristol, Avon)*, 2005. 20(10): p. 1101-10

[39] Chang CY, Rupp JD, Reed MP, Hughes RE, and Schneider LW. Predicting the effects of muscle activation on knee, thigh, and hip injuries in frontal crashes using a finite-element model with muscle forces from subject testing and musculoskeletal modeling. *Stapp Car Crash J*, 2009. 53: p. 291-328
[40] Bose D and Crandall JR. Influence of active muscle contribution on the injury response of restrained car occupants. 2008. p. 61-72.
[41] Murphy DF, Connolly DA, and Beynnon BD. Risk factors for lower extremity injury: a review of the literature. *Br J Sports Med*, 2003. 37(1): p. 13-29
[42] Finestone A, Milgrom C, et al. Overuse injuries in female infantry recruits during low-intensity basic training. *Med Sci Sports Exerc*, 2008. 40(11 Suppl): p. S630-5
[43] Harm DL, Jennings RT, et al. Invited review: gender issues related to spaceflight: a NASA perspective. *J Appl Physiol (1985)*, 2001. 91(5): p. 2374-83

VIII. APPENDIX

Appendix A: PMHS Lumped Parameter Model Parameters

TABLE AI
PMHS MODELS

Model Parameter	50th Male PMHS [3]	PMHS 1 [1]	PMHS 2 [1]	PMHS 3 [1]	PMHS 4 [1]
mA	2.2 kg	1.180 kg	1.009 kg	1.288 kg	0.886 kg
mB	3.1 kg	0.742 kg	0.626 kg	0.576 kg	0.650 kg
mC	4.6 kg	4.527 kg	6.725 kg	5.916 kg	4.815 kg
mD	0.001 kg	1.879 kg	2.218 kg	2.830 kg	1.746 kg
mE	25 kg	10.659 kg	12.927 kg	10.885 kg	8.618 kg
mF	5.0 kg	1.121 kg	1.745 kg	1.486 kg	0.846 kg
mG	0.001 kg	0.273 kg	0.301 kg	0.263 kg	0.294 kg
mH	N/A	1.121 kg	1.745 kg	1.486 kg	0.846 kg
kAG	425,000 N/m	457768 N/m	572456 N/m	441384 N/m	490536 N/m
cAG	1,500 Ns/m	2364 Ns/m	4316 Ns/m	5340 Ns/m	1468 Ns/m
kGB	55,000 N/m	444120 N/m	38616 N/m	661208 N/m	259800 N/m
cGB	10,690 Ns/m	1904 Ns/m	3120 Ns/m	976 Ns/m	1040 Ns/m
kBC	128,420 N/m	141034 N/m	187114 N/m	88810 N/m	3050 N/m
cBC	1,000 Ns/m	1184 Ns/m	1080 Ns/m	1064 Ns/m	2616 Ns/m
kAD	100,000 N/m	15 N/m	15 N/m	15 N/m	11 N/m
cAD	50,000 Ns/m	195 Ns/m	220 Ns/m	204 Ns/m	236 Ns/m
kBE	70 N/m	7 N/m	7 N/m	7 N/m	15 N/m
cBE	30 Ns/m	203 Ns/m	155 Ns/m	34 Ns/m	29 Ns/m
kAF	128,190 N/m	62654 N/m	101566 N/m	48318 N/m	59582 N/m
cAF	500 Ns/m	116 Ns/m	212 Ns/m	148 Ns/m	108 Ns/m
kGH	N/A	62654 N/m	101566 N/m	48318 N/m	59582 N/m
cGH	N/A	116 Ns/m	212 Ns/m	148 Ns/m	108 Ns/m

Appendix B: Hybrid III 5th Percentile Female Lumped Parameter Model Parameters and Validation

TABLE BI
HYBRID III MODELS

Model Parameter	Hybrid III 50th Male [6]	Hybrid III 5th Female
mA	6.68 kg	1.7526 kg
mB	7.11 kg	4.4838 kg
mC	0.001 kg	0.001 kg
mD	0.5 kg	0.3153 kg
mE	5.4 kg	3.4054 kg
mF	0.9 kg	0.5676 kg
mG	0.001 kg	2.46 kg
mH	N/A	0.001 kg

kAG	3,000,000 N/m	3,000,000 N/m
cAG	25,000 Ns/m	25,000 Ns/m
kGB	3,000,000 N/m	3,000,000 N/m
cGB	30,000 Ns/m	30,000 Ns/m
kBC	1,000,000 N/m	1,000,000 N/m
cBC	25,000 Ns/m	25,000 Ns/m
kAD	13,520,000 N/m	13,520,000 N/m
cAD	1,000 Ns/m	1,000 Ns/m
kBE	500 N/m	500 N/m
cBE	1,500 Ns/m	1,500 Ns/m
kAF	100,000 N/m	100,000 N/m
cAF	25,000 Ns/m	25,000 Ns/m
kGH	N/A	100,000 N/m
cGH	N/A	25,000 Ns/m

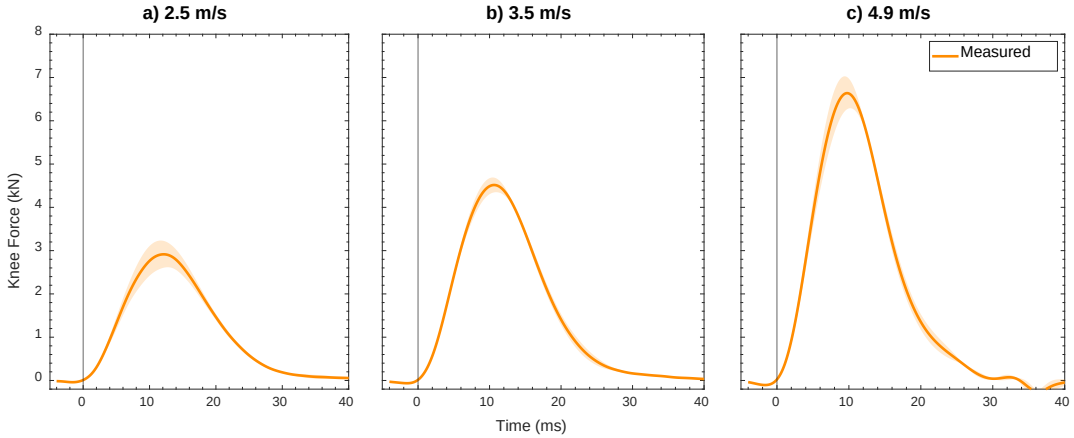

Fig. B1. Knee force recorded by averaging the left and right impactor load cells for all a) 2.5 m/s, b) 3.5 m/s, and c) 4.9 m/s impacts on the Hybrid III 5th Percentile Female. Results are shown as the average knee force ± one standard deviation.

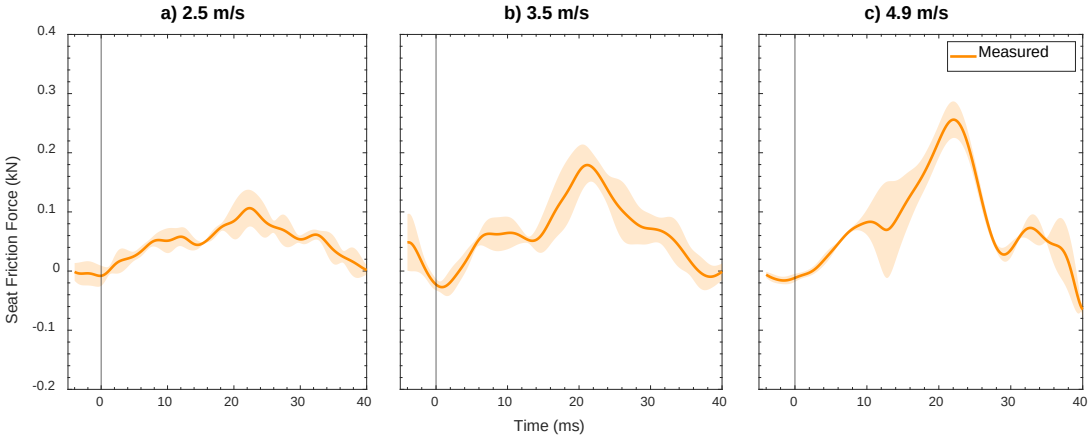

Fig. B2. Friction force recorded by the seat load cell for all a) 2.5 m/s, b) 3.5 m/s, and c) 4.9 m/s impacts on the Hybrid III 5th Percentile Female. Results are shown as the average seat friction force ± one standard deviation.

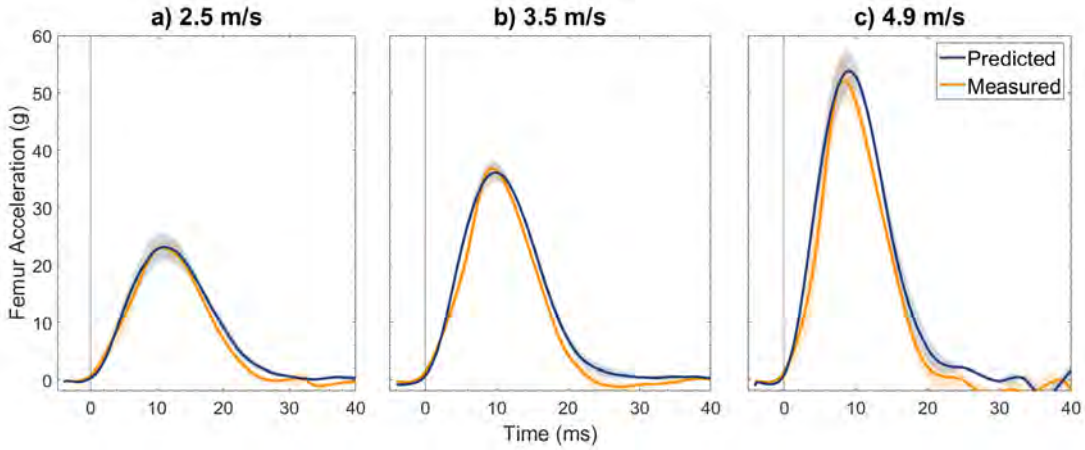

Fig. B3. Prediction of femur acceleration (in multiples of gravity) via the lumped parameter model compared with the acceleration recorded by the femur accelerometer for all a) 2.5 m/s, b) 3.5 m/s, and c) 4.9 m/s impacts on the Hybrid III 5th Percentile Female. Results are shown as the average femur acceleration ± one standard deviation.

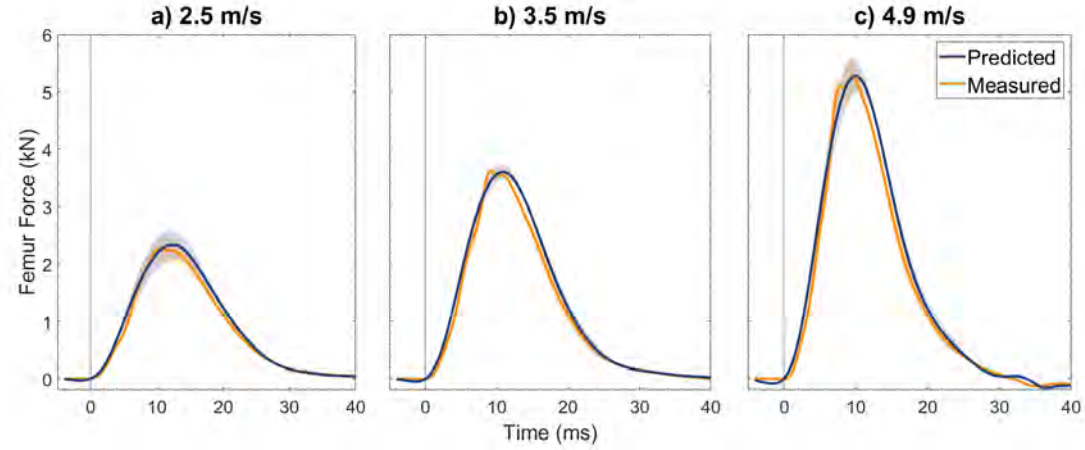

Fig. B4. Prediction of femur force (in kN) via the lumped parameter model compared with the force recorded by the femur load cell for all a) 2.5 m/s, b) 3.5 m/s, and c) 4.9 m/s impacts on the Hybrid III 5th Percentile Female. Results are shown as the average femur force ± one standard deviation.

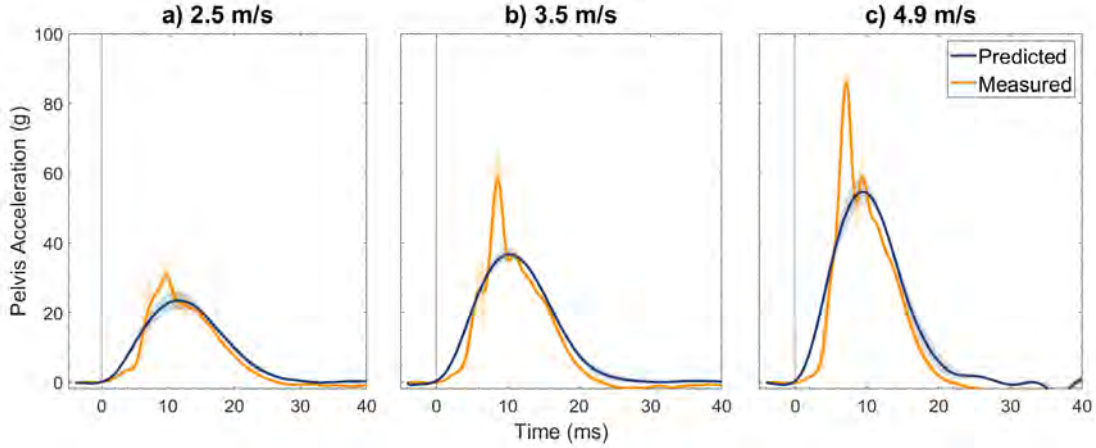

Fig. B5. Prediction of pelvis acceleration (in multiples of gravity) via the lumped parameter model compared with the acceleration recorded by the pelvis accelerometer for all a) 2.5 m/s, b) 3.5 m/s, and c) 4.9 m/s impacts on the Hybrid III 5th Percentile Female. Results are shown as the average pelvis acceleration ± one standard deviation.

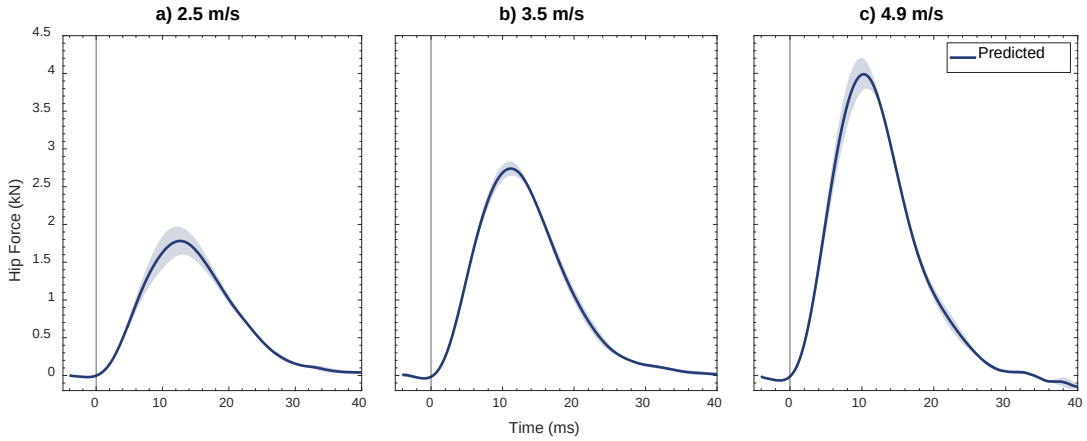

Fig. B6. Average predicted hip force (in kN) via the lumped parameter model for all a) 2.5 m/s, b) 3.5 m/s, and c) 4.9 m/s impacts on the Hybrid III 5th Percentile Female. Results are shown as the average hip force ± one standard deviation.

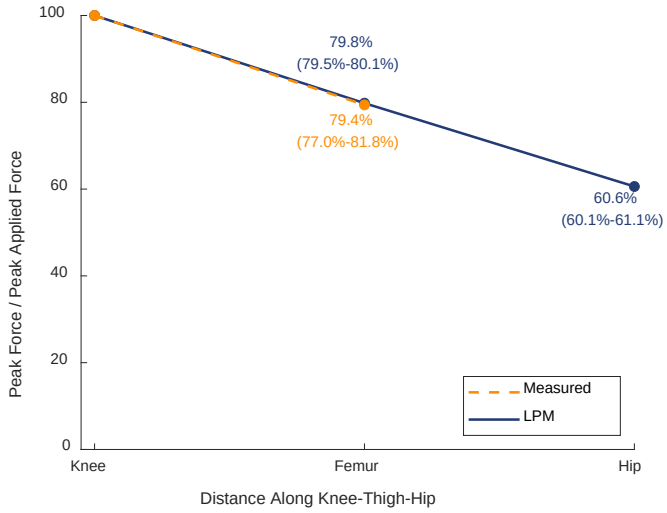

Fig. B7. Average force transfer predicted and measured along KTH (± one standard deviation) for the Hybrid III 5th Percentile Female.

Appendix C: Input Loading Characteristics

TABLE CI
KNEE LOADING CHARACTERISTICS FOR PMHS TESTS

Impact Velocity (m/s)	Subject	Loading Rate (N/ms)	Loading Duration (ms)	Impulse of Loading (J)	Time to Maximum Force (ms)	Maximum force (kN)
2.5	1	258	33.2	43.4	12.5	2.10
	2	253	33.4	51.2	14.6	2.44
	3	220	39.6	54.0	15.8	2.29
	4	256	29.7	36.5	12.0	1.98
	Average (±SD)	247 (±18)	34.0 (±4.1)	46.3 (±7.9)	13.7 (±1.8)	2.20 (±0.20)
3.5	1	432	29.5	57.0	11.1	3.09
	2	388	30.5	66.8	14.2	3.47
	3	407	33.1	69.5	13.1	3.52
	4	430	25.7	48.8	10.6	2.96
	Average (±SD)	414 (±21)	29.7 (±3.1)	60.6 (±9.5)	12.3 (±1.7)	3.26 (±0.28)
4.9	1	659	21.5	71.6	8.5	3.83
	2	680	24.3	83.5	8.6	3.95

	3	612	25.1	83.5	9.5	3.88
	4	658	21.8	62.9	8.1	3.63
	Average (±SD)	659 (±16)	24.8 (±1.3)	75.4 (±10.0)	11.0 (±0.5)	4.71 (±0.50)

TABLE CII
KNEE LOADING CHARACTERISTICS FOR HYBRID III TESTS

Impact Velocity (m/s)	Test	Loading Rate (N/ms)	Loading Duration (ms)	Impulse of Loading (J)	Time to Maximum Force (ms)	Maximum force (kN)
2.5	1	397	23.2	44.6	11.5	3.18
	2	367	24.1	45.1	12.4	3.02
	3	295	24.4	39.1	12.7	2.58
	Average (±SD)	353 (±52)	23.9 (±0.6)	43.0 (±3.3)	12.2 (±0.6)	2.92 (±0.31)
3.5	1	658	20.0	57.8	10.5	4.70
	2	631	21.4	59.2	10.6	4.50
	3	589	21.8	58.5	11.0	4.36
	Average (±SD)	626 (±35)	21.1 (±0.9)	58.5 (±0.7)	10.7 (±0.3)	4.52 (±0.17)
4.9	1	1072	18.6	78.0	9.4	7.01
	2	1008	19.2	76.6	9.7	6.67
	3	878	20.8	76.8	10.2	6.28
	Average (±SD)	986 (±99)	19.5 (±1.1)	77.1 (±0.8)	9.8 (±0.4)	6.65 (±0.36)

TABLE CIII
KNEE LOADING CHARACTERISTICS FOR THOR TESTS

Impact Velocity (m/s)	Test	Loading Rate (N/ms)	Loading Duration (ms)	Impulse of Loading (J)	Time to Maximum Force (ms)	Maximum force (kN)
2.5	1	307	26.4	44.1	12.9	2.64
	2	279	27.7	44.1	13.4	2.55
	3	299	27.0	45.7	13.4	2.70
	Average (±SD)	295 (±14)	27.0 (±0.7)	44.6 (±0.9)	13.2 (±0.3)	2.63 (±0.08)
3.5	1	495	24.5	60.9	12.1	4.01
	2	541	24.2	62.5	11.5	4.16
	3	510	24.7	62.6	11.9	4.09
	Average (±SD)	515 (±24)	24.5 (±0.3)	62.0 (±0.9)	11.8 (±0.3)	4.09 (±0.07)
4.9	*1*	829	22.3	81.6	10.7	6.10

Appendix D: Femur Kinematics

TABLE DI
MEASURED PMHS FEMUR KINEMATICS

Impact Velocity (m/s)	Subject	Maximum Femur Acceleration (g)	Time to Maximum Femur Acceleration (ms)
2.5	1	24.6	7.2
	2	16.5	10.7
	3	20.8	8
	4	24.6	5.8
	Average (± SD)	21.6 (±3.9)	7.9 (±2.1)
3.5	1	33.6	4.9
	2	24.3	8.1

	3	34.6	6.4
	4	38.2	4.9
	Average (± SD)	32.7 (±5.9)	6.1 (±1.5)
4.9	1	48.5	5.6
	2	41.5	6.5
	3	53.4	5.2
	4	53.4	5.0
	Average (± SD)	49.2 (±5.6)	5.6 (±0.7)

TABLE DII
MEASURED HYBRID III FEMUR KINEMATICS

Impact Velocity (m/s)	Test	Maximum Femur Acceleration (g)	Time to Maximum Femur Acceleration (ms)
2.5	1	23.4	11.9
	2	24.1	10.6
	3	21.7	10.2
	Average (± SD)	23.1 (±1.2)	10.9 (±0.9)
3.5	1	35.8	9.8
	2	38.8	9.2
	3	36.3	9.2
	Average (± SD)	37.0 (±1.6)	9.4 (±0.3)
4.9	1	56.7	8.3
	2	50.8	8.3
	3	49.2	8.5
	Average (± SD)	52.2 (±4.0)	8.4 (±0.1)

TABLE DIII
MEASURED THOR FEMUR KINEMATICS

Impact Velocity (m/s)	Test	Maximum Femur Acceleration (g)	Time to Maximum Femur Acceleration (ms)
2.5	1	21.2	10.4
	2	20.1	10.9
	3	21.1	10.8
	Average (± SD)	20.8 (±0.6)	10.7 (±0.3)
3.5	1	33.1	9.7
	2	35.3	9.1
	3	34.1	9.4
	Average (± SD)	34.2 (±1.1)	9.4 (±0.3)
4.9	1	51.3	8.5

Appendix E: Femur Loading

TABLE EI
PREDICTED FEMUR LOADING CHARACTERISTICS FOR PMHS TESTS

Impact Velocity (m/s)	Subject	Loading Rate (N/ms)	Loading Duration (ms)	Impulse of Loading (J)	Time to Maximum Force (ms)	Maximum force (kN)
2.5	1	165	34.0	33.4	15.1	1.52
	2	171	34.4	39.3	16.8	1.76
	3	152	38.1	37.5	16.7	1.58
	4	164	28.3	26.2	13.6	1.42
	Average (±SD)	163 (±8)	33.7 (±4.0)	34.1 (±5.8)	15.6 (±1.5)	1.57 (±0.14)

3.5	1	279	30.5	43.7	13.1	2.20
	2	255	31.7	51.0	16.0	2.48
	3	272	33.0	48.1	13.9	2.41
	4	273	25.2	35.5	12.4	2.13
	Average (±SD)	270 (±10)	30.1 (±3.4)	44.6 (±6.8)	13.9 (±1.6)	2.31 (±0.17)
4.9	1	421	26.4	54.6	12.2	3.12
	2	435	25.9	63.2	12.6	3.57
	3	450	27.0	57.4	12.0	3.42
	4	420	23.3	46.0	12.1	2.97
	Average (±SD)	432 (±14)	25.7 (±1.6)	55.3 (±7.1)	12.2 (±0.3)	3.27 (±0.28)

TABLE EII
MEASURED FEMUR LOADING CHARACTERISTICS FOR HYBRID III TESTS

Impact Velocity (m/s)	Test	Loading Rate (N/ms)	Loading Duration (ms)	Impulse of Loading (J)	Time to Maximum Force (ms)	Maximum force (kN)
2.5	1	359	23.4	33.4	11.5	2.39
	2	303	24.1	34.2	10.5	2.42
	3	238	24.3	30.0	9.9	2.04
	Average (±SD)	300 (±60)	23.9 (±0.5)	32.5 (±2.2)	10.6 (±0.8)	2.28 (±0.21)
3.5	1	586	19.7	42.5	9.4	3.61
	2	477	20.9	45.2	9.2	3.68
	3	467	21.1	44.0	9.0	3.62
	Average (±SD)	510 (±66)	20.6 (±0.8)	43.9 (±1.3)	9.2 (±0.2)	3.63 (±0.04)
4.9	1	950	18.1	57.9	9.3	5.61
	2	898	18.8	57.7	9.4	5.27
	3	766	20.2	58.1	9.9	5.03
	Average (±SD)	871 (±95)	19.0 (±1.1)	57.9 (±0.2)	9.5 (±0.3)	5.30 (±0.29)

TABLE EIII
MEASURED FEMUR LOADING CHARACTERISTICS FOR THOR TESTS

Impact Velocity (m/s)	Test	Loading Rate (N/ms)	Loading Duration (ms)	Impulse of Loading (J)	Time to Maximum Force (ms)	Maximum force (kN)
2.5	1	212	26.2	35.8	12.9	2.19
	2	199	27.4	36.0	13.6	2.12
	3	212	26.7	37.2	13.4	2.25
	Average (±SD)	207 (±7)	26.8 (±0.6)	36.3 (±0.7)	13.3 (±0.4)	2.19 (±0.06)
3.5	1	354	23.7	48.0	12.6	3.33
	2	398	23.5	49.4	11.9	3.42
	3	375	24.1	49.9	12.0	3.37
	Average (±SD)	376 (±22)	23.8 (±0.3)	49.1 (±0.9)	12.2 (±0.4)	3.37 (±0.05)
4.9	*1*	624	21.0	62.7	11.1	5.03

Appendix F: Pelvis Kinematics

TABLE FI
MEASURED PMHS PELVIS TRANSLATIONAL KINEMATICS

Impact Velocity (m/s)	Subject	Maximum Pelvis Acceleration (g)	Time to Maximum Pelvis Acceleration (ms)

2.5	1	30.1	7.7
	2	12.3	9.8
	3	19.9	10.9
	4	35.4	10.1
	Average (± SD)	24.4 (±10.4)	9.6 (±1.4)
3.5	1	45.6	6.7
	2	18.8	9.2
	3	30.8	8.6
	4	48.7	8.6
	Average (± SD)	36.0 (±13.9)	8.3 (±1.1)
4.9	1	61.7	6.5
	2	30.2	7.0
	3	44.9	7.2
	4	62.4	7.9
	Average (± SD)	49.8 (±15.3)	7.2 (±0.6)

TABLE FII
MEASURED PMHS PELVIS ROTATIONAL KINEMATICS

Impact Velocity (m/s)	Subject	Pelvis Angular Displacement at Maximum Knee Force (deg)	Time of Maximum Knee Force (ms)	Maximum Pelvis Angular Displacement (deg)	Time to Maximum Pelvis Angular Displacement (ms)
2.5	1	0.8	12.5	25.1	105.9
	2	-2.2	14.6	22.6	96.2
	3	-1.1	15.8	24.0	75.9
	4	-1.2	12.0	33.1	91.4
	Average (± SD)	-0.9 (±1.3)	13.7 (±1.8)	26.2 (±4.7)	92.4 (±12.5)
3.5	1	0.3	11.1	25.9	83.4
	2	-3.2	14.2	34.8	71.3
	3	-2.9	13.1	31.2	72.8
	4	-2.0	10.6	33.4	61.0
	Average (± SD)	-1.9 (±1.6)	12.3 (±1.7)	31.3 (±3.9)	72.1 (±9.2)
4.9	1	-0.2	10.7	27.8	69.6
	2	-4.6	11.4	42.1	62.1
	3	-4.5	11.4	36.2	44.6
	4	-2.8	10.4	44.9	58.1
	Average (± SD)	-3.0 (±2.1)	11.0 (±0.5)	37.7 (±7.5)	58.6 (±10.5)

TABLE FIII
MEASURED HYBRID III PELVIS TRANSLATIONAL KINEMATICS

Impact Velocity (m/s)	Test	Maximum Pelvis Acceleration (g)	Time to Maximum Pelvis Acceleration (ms)
2.5	1	27.3	9.7
	2	35.1	10.0
	3	32.4	9.3
	Average (± SD)	31.6 (±3.9)	9.7 (±0.4)
3.5	1	50.6	8.9
	2	59.9	8.5
	3	67.2	8.6
	Average (± SD)	59.2 (±8.3)	8.7 (±0.2)

4.9	1	89.9	6.9
	2	87.8	7.1
	3	88.7	7.4
	Average (± SD)	88.8 (±1.1)	7.1 (±0.3)

TABLE FIV
MEASURED HYBRID III PELVIS ROTATIONAL KINEMATICS

Impact Velocity (m/s)	Test	Pelvis Angular Displacement at Maximum Knee Force (deg)	Time of Maximum Knee Force (ms)	Maximum Pelvis Angular Displacement (deg)	Time to Maximum Pelvis Angular Displacement (ms)
2.5	1	0.6	11.5	21.9	81.1
	2	0.8	12.4	22.8	77.9
	3	0.8	12.7	21.6	93.2
	Average (± SD)	0.7 (±0.1)	12.2 (±0.6)	22.1 (±0.6)	84.1 (±8.1)
3.5	1	0.8	10.5	24.9	62.6
	2	0.9	10.6	26.4	64.3
	3	0.9	11.0	25.8	66.1
	Average (± SD)	0.9 (±0.0)	10.7 (±0.3)	25.7 (±0.8)	64.3 (±1.8)
4.9	1	1.0	9.4	28.1	52.9
	2	1.0	9.7	28.3	54.9
	3	1.0	10.2	28.9	56.4
	Average (± SD)	1.0 (±0.0)	9.8 (±0.4)	28.4 (±0.4)	54.7 (±1.8)

TABLE FV
MEASURED THOR PELVIS TRANSLATIONAL KINEMATICS

Impact Velocity (m/s)	Test	Maximum Pelvis Acceleration (g)	Time to Maximum Pelvis Acceleration (ms)
2.5	1	25.0	10.3
	2	25.7	11.0
	3	25.0	10.9
	Average (± SD)	25.2 (±0.4)	10.7 (±0.4)
3.5	1	38.2	10.2
	2	41.8	9.3
	3	38.4	9.5
	Average (± SD)	39.5 (±2.0)	9.7 (±0.5)
4.9	1	59.1	8.7

TABLE FVI
MEASURED THOR PELVIS ROTATIONAL KINEMATICS

Impact Velocity (m/s)	Test	Pelvis Angular Displacement at Maximum Knee Force (deg)	Time of Maximum Knee Force (ms)	Maximum Pelvis Angular Displacement (deg)	Time to Maximum Pelvis Angular Displacement (ms)
2.5	1	0.4	12.9	24.3	107.2
	2	0.4	13.4	24.6	108.6
	3	0.4	13.4	24.9	105.4
	Average (± SD)	0.4 (±0.0)	13.2 (±0.3)	24.6 (±0.3)	107.1 (±1.6)

3.5	1	0.6	12.1	25.5	81.1
	2	0.6	11.5	24.4	79.0
	3	0.6	11.9	24.8	80.3
	Average (± SD)	0.6 (±0.0)	11.8 (±0.3)	24.9 (±0.6)	80.1 (±1.1)
4.9	1	0.9	10.7	26.3	64.3

Appendix G: Hip Loading

TABLE GI
PREDICTED HIP LOADING CHARACTERISTICS FOR PMHS TESTS

Impact Velocity (m/s)	Subject	Loading Rate (N/ms)	Loading Duration (ms)	Impulse of Loading (J)	Time to Maximum Force (ms)	Maximum force (kN)
2.5	1	125	35.2	29.9	19.2	1.28
	2	123	36.2	34.3	20.8	1.47
	3	119	39.8	32.0	17.3	1.24
	4	125	29.0	22.7	15.4	1.18
	Average (±SD)	123 (±3)	35.1 (±4.5)	29.7 (±5.0)	18.2 (±2.3)	1.29 (±0.12)
3.5	1	215	32.6	39.3	14.0	1.79
	2	177	33.5	44.4	18.3	2.00
	3	212	34.9	40.7	14.0	1.87
	4	213	26.0	30.7	13.4	1.75
	Average (±SD)	204 (±18)	31.8 (±3.9)	38.8 (±5.8)	14.9 (±2.3)	1.85 (±0.11)
4.9	1	332	28.2	48.7	13.2	2.50
	2	304	28.7	54.9	16.4	2.78
	3	355	28.9	48.0	12.1	2.65
	4	331	24.2	39.8	13.5	2.43
	Average (±SD)	330 (±21)	27.5 (±2.2)	47.8 (±6.2)	13.8 (±1.8)	2.59 (±0.16)

TABLE GII
PREDICTED HIP LOADING CHARACTERISTICS FOR HYBRID III TESTS

Impact Velocity (m/s)	Test	Loading Rate (N/ms)	Loading Duration (ms)	Impulse of Loading (J)	Time to Maximum Force (ms)	Maximum force (kN)
2.5	1	238	23.8	28.3	12.1	1.94
	2	218	24.7	28.2	12.8	1.84
	3	170	25.8	24.7	13.1	1.58
	Average (±SD)	209 (±35)	24.8 (±1.0)	27.1 (±2.0)	12.7 (±0.5)	1.79 (±0.19)
3.5	1	387	21.0	36.2	11.1	2.84
	2	378	22.3	37.3	11.0	2.73
	3	349	22.5	36.8	11.4	2.65
	Average (±SD)	371 (±20)	21.9 (±0.8)	36.8 (±0.5)	11.2 (±0.2)	2.74 (±0.09)
4.9	1	628	20.1	49.4	9.9	4.19
	2	587	20.6	48.4	10.2	4.01
	3	521	21.7	48.0	10.7	3.79
	Average (±SD)	579 (±54)	20.8 (±0.8)	48.6 (±0.7)	10.3 (±0.4)	4.00 (±0.20)

TABLE GIII
MEASURED HIP LOADING CHARACTERISTICS FOR THOR TESTS

Impact Velocity (m/s)	Test	Loading Rate (N/ms)	Loading Duration (ms)	Impulse of Loading (J)	Time to Maximum Force (ms)	Maximum force (kN)
2.5	1	126	26.2	18.2	13.4	1.11
	2	116	27.5	18.2	14.7	1.05
	3	123	26.7	18.7	14.1	1.12
	Average (±SD)	121 (±5)	26.8 (±0.7)	18.4 (±0.3)	14.1 (±0.7)	1.10 (±0.04)
3.5	1	212	23.4	24.4	12.9	1.68
	2	232	23.6	25.0	12.8	1.71
	3	235	24.3	25.4	12.9	1.68
	Average (±SD)	226 (±12)	23.8 (±0.5)	24.9 (±0.5)	12.9 (±0.1)	1.69 (±0.02)
4.9	*1*	396	21.4	31.9	12.0	2.50

Appendix H: Force and Impulse Transfer

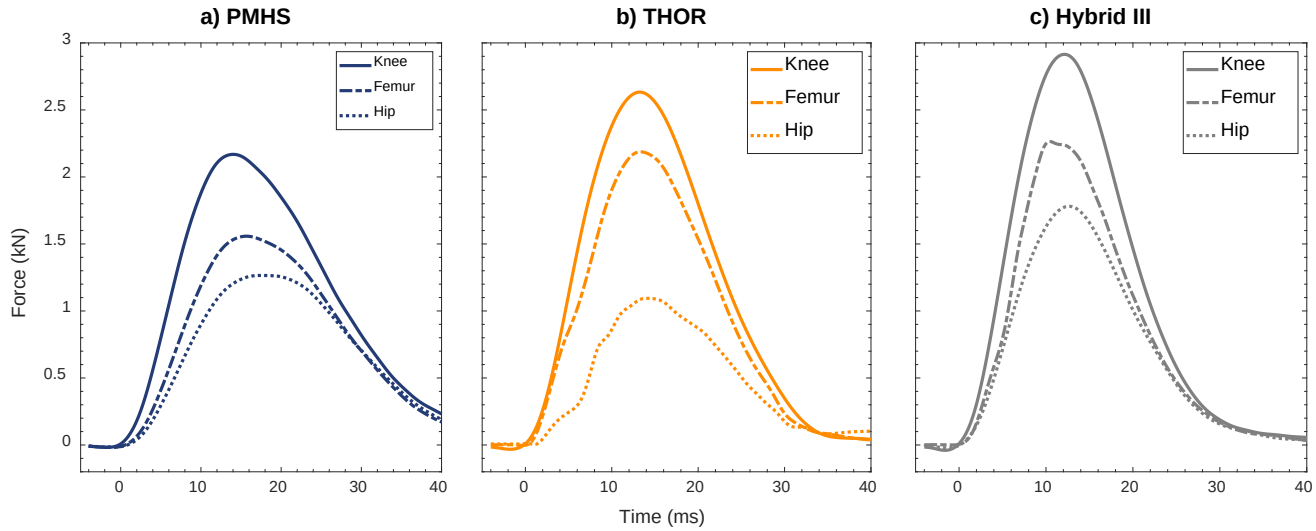

Fig. H1. Average force transfer measured/predicted for a) PMHS, b) THOR, and c) Hybrid III for the 2.5 m/s impact velocity.

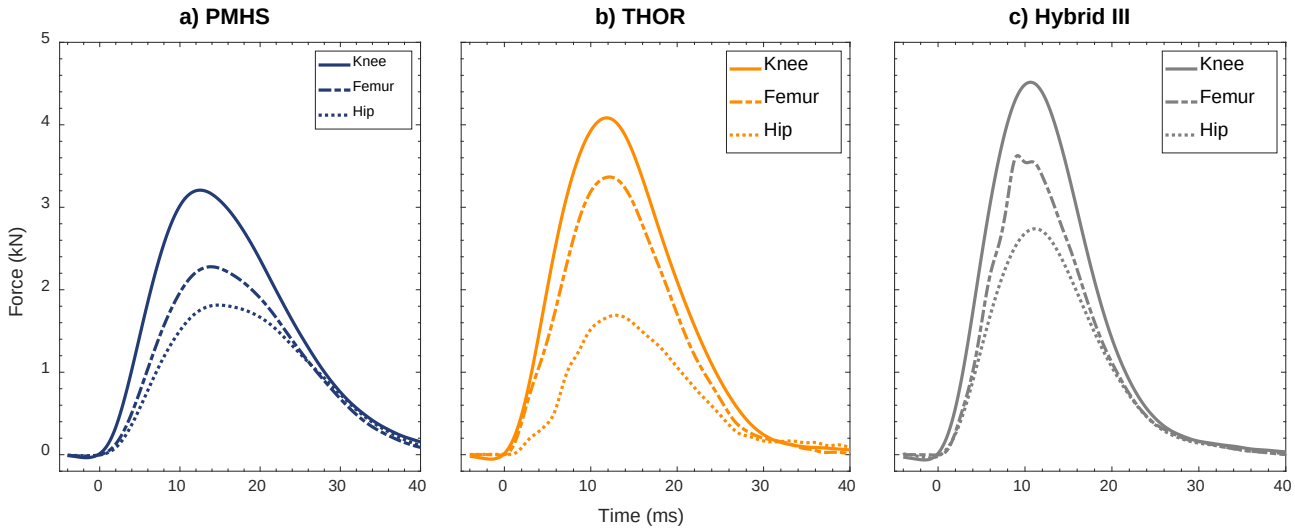

Fig. H2. Average force transfer measured/predicted for a) PMHS, b) THOR, and c) Hybrid III for the 3.5 m/s impact velocity.

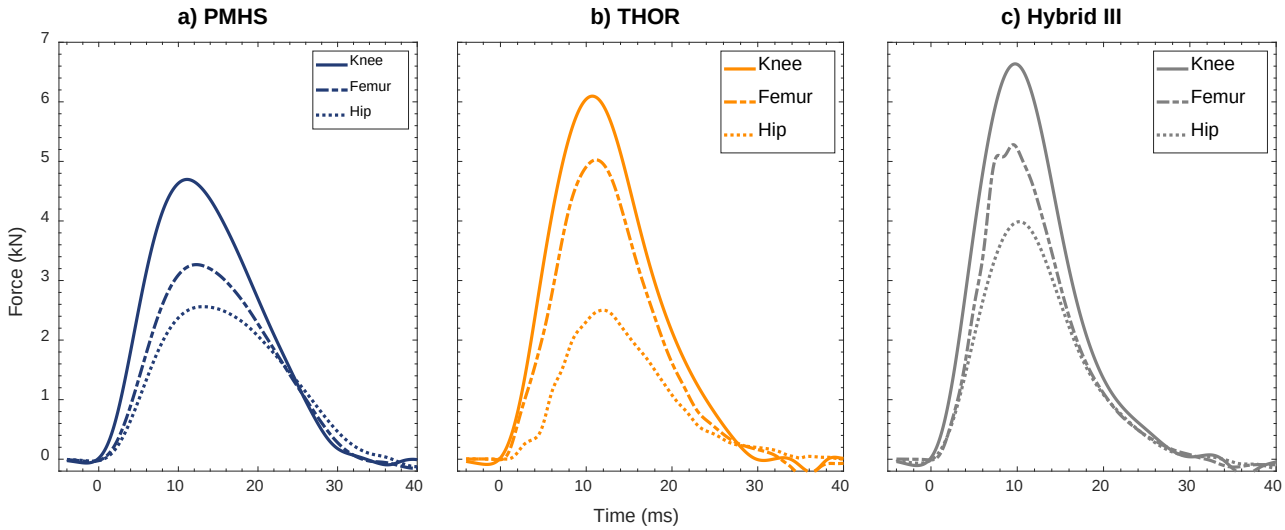

Fig. H3. Average force transfer measured/predicted for a) PMHS, b) THOR, and c) Hybrid III for the 4.9 m/s impact velocity.

TABLE HI
PREDICTED PMHS FORCE TRANSFER

Impact Velocity (m/s)	Subject	Predicted Femur Force Transfer (%)	Predicted Hip Force Transfer (%)
2.5	1	72.1	61.0
	2	72.1	60.2
	3	69.0	54.0
	4	72.1	59.8
	Average (± SD)	71.3 (±1.6)	58.8 (±3.2)
3.5	1	71.3	58.0
	2	71.5	57.7
	3	68.3	53.1
	4	72.2	59.2
	Average (± SD)	70.9 (±1.7)	57.0 (±2.7)
4.9	1	70.2	56.3
	2	69.4	53.9
	3	67.1	51.9
	4	71.6	58.7
	Average (± SD)	69.6 (±1.9)	55.2 (±2.9)
PMHS Average (± SD)		70.6 (±1.7)	57.0 (±3.0)

TABLE HII
MEASURED/PREDICTED HYBRID III FORCE TRANSFER

Impact Velocity (m/s)	Test	Measured Femur Force Transfer (%)	Predicted Hip Force Transfer (%)
2.5	1	75.1	61.0
	2	80.2	61.0
	3	79.0	61.2
	Average (± SD)	78.1 (±2.6)	61.1 (±0.1)
3.5	1	76.8	60.5
	2	81.7	60.6
	3	83.0	60.9
	Average (± SD)	80.5 (±3.3)	60.7 (±0.2)
4.9	1	80.0	59.8
	2	79.0	60.1

	3	80.0	60.3
	Average (± SD)	79.7 (±0.6)	60.1 (±0.3)
Hybrid III Average (± SD)		79.4 (±2.4)	60.6 (±0.5)

TABLE HIII
MEASURED THOR FORCE TRANSFER

Impact Velocity (m/s)	Test	Measured Femur Force Transfer (%)	Measured Hip Force Transfer (%)
2.5	1	83.0	41.8
	2	83.1	41.3
	3	83.2	41.6
	Average (± SD)	83.1 (±0.1)	41.6 (±0.3)
3.5	1	82.9	41.9
	2	82.3	41.1
	3	82.3	41.1
	Average (± SD)	82.5 (±0.4)	41.4 (±0.5)
4.9	1	82.5	41.1
THOR Average (± SD)		82.7 (±0.4)	41.4 (±0.4)

TABLE HIV
FORCE TRANSFER RELATIONSHIPS BETWEEN ATDS AND PMHS

ATD Location	PMHS Femur (Current Test Conditions)	PMHS Hip (Current Test Conditions)	PMHS Femur (Equal Knee Forces)	PMHS Hip (Equal Knee Forces)
Hybrid III Femur	1.55	1.92	1.12	1.39
Hybrid III Hip	1.18	1.46	0.86	1.06
THOR Femur	1.46	1.81	1.17	1.45
THOR Hip	0.73	0.91	0.59	0.73

TABLE HV
PREDICTED PMHS IMPULSE TRANSFER

Impact Velocity (m/s)	Subject	Predicted Femur Impulse Transfer (%)	Predicted Hip Impulse Transfer (%)
2.5	1	76.9	69.0
	2	76.8	67.0
	3	69.4	59.2
	4	71.7	62.2
	Average (± SD)	73.7 (±3.8)	64.3 (±4.5)
3.5	1	76.6	68.9
	2	76.4	66.4
	3	69.2	58.6
	4	72.7	62.9
	Average (± SD)	73.7 (±3.5)	64.2 (±4.5)
4.9	1	76.2	68.0
	2	75.7	65.7
	3	68.8	57.5
	4	73.2	63.3
	Average (± SD)	73.5 (±3.4)	63.6 (±4.5)
PMHS Average (± SD)		73.6 (±3.2)	64.1 (±4.1)

TABLE HVI
MEASURED/PREDICTED HYBRID III IMPULSE TRANSFER

Impact Velocity (m/s)	Test	Measured Femur Impulse Transfer (%)	Predicted Hip Impulse Transfer (%)
2.5	1	74.8	63.4
	2	75.8	62.4
	3	76.6	63.2
	Average (± SD)	75.8 (±0.9)	63.0 (±0.5)
3.5	1	73.6	62.8
	2	76.2	62.9
	3	75.2	62.9
	Average (± SD)	75.0 (±1.3)	62.8 (±0.1)
4.9	1	74.2	63.3
	2	75.4	63.2
	3	75.6	62.4
	Average (± SD)	75.1 (±0.8)	63.0 (±0.5)
Hybrid III Average (± SD)		75.3 (±1.0)	62.9 (±0.4)

TABLE HVII
MEASURED THOR IMPULSE TRANSFER

Impact Velocity (m/s)	Test	Measured Femur Impulse Transfer (%)	Measured Hip Impulse Transfer (%)
2.5	1	81.2	41.2
	2	81.7	41.2
	3	81.3	41.0
	Average (± SD)	81.4 (±0.3)	41.1 (±0.1)
3.5	1	78.8	40.0
	2	79.0	40.0
	3	79.6	40.6
	Average (± SD)	79.2 (±0.4)	40.2 (±0.3)
4.9	1	76.8	39.0
THOR Average (± SD)		79.8 (±1.7)	40.4 (±0.8)